

# **Theory of Fission Neutron Multiplicities and Implementation in MCNPX-PoliMi**

**Theorie der Multiplizitätsverteilung von Spaltneutronen und deren Implementierung in  
MCNPX-PoliMi**

von  
Fabio Zeiser  
geboren am 20.09.1990

Zentrum für Naturwissenschaften und Friedensforschung

Bachelor-Arbeit im Studiengang Physik  
Universität Hamburg  
August 2013

1. Gutachter: Prof. Gerald Kirchner
  2. Gutachter: Prof. Götz Neuneck
- Betreuer: Malte Göttsche



---

Hiermit bestätige ich, dass die vorliegende Arbeit von mir selbständig verfasst wurde und ich keine anderen als die angegebenen Hilfsmittel – insbesondere keine im Quellenverzeichnis nicht benannten Internet-Quellen – benutzt habe und die Arbeit von mir vorher nicht einem anderen Prüfungsverfahren eingereicht wurde. Die eingereichte schriftliche Fassung entspricht der auf dem elektronischen Speichermedium. Ich bin damit einverstanden, dass die Bachelorarbeit veröffentlicht wird.

Hamburg, den 23. August 2013



## Zusammenfassung

Die Messung von Neutronenmultiplizitäten ist eine wichtige Technik zur Bestimmung der Masse nuklearer Materialien. Sie benötigt genaue Kenntnis der Emissionswahrscheinlichkeit von Spaltneutronen. Diese Studie fasst das Verständnis der physikalischen Ursache von Neutronenmultiplizitäten zusammen und untersucht deren Implementierung in MCNPX-PoliMi. Insbesondere werden dabei auch verschiedene Ansätze verglichen, wie die Energie der einfallenden Teilchen zu berücksichtigen ist.

Um erklären zu können warum Spaltfragmente Neutronen emittieren wird Weisskopfs Verdampfungstheorie aufgegriffen. Sie bestimmt die Emissionswahrscheinlichkeit als Funktion der Anregungsenergie der Fragmente. Aus der Theorie folgt zudem, mit einigen Zusätzen, eine Maxwell-Energieverteilung im Schwerpunktsystem für die emittierten Neutronen. Weiterhin werden die Berechnungen von Leachman vorgestellt, welcher empirische Daten nutzt um die Anregungsenergien zu bestimmen und schließlich die Ergebnisse der Verdampfungstheorie zur Ermittlung der Multiplizitätsverteilung verwendet.

Mit nur zwei Annahmen zeigt Terrell, dass die Multiplizitäten durch eine Gauß-Funktion angenähert werden können. Dies ist die erste von zwei Optionen mit welcher Neutronenmultiplizitäten in MCNPX-PoliMi simuliert werden können. Für die zweite Option wird angenommen<sup>1</sup>, dass Zucker und Holdens Auswertung für ein Experiment implementiert ist mit  $^{235}\text{U}$ ,  $^{238}\text{U}$  and  $^{239}\text{Pu}$  im Energiebereich der einfallenden Neutronen zwischen 0 und 10 MeV.

Schließlich folgt, für ein vereinfachtes System, die Entwicklung einer quantitativen Beschreibung der Abweichungen zwischen den Emissionswahrscheinlichkeiten, wie sie von Terrell vorhergesagt werden, und jenen Messung von Zucker und Holden. Das Ergebnis dieser Studie deutet auf eine Abweichung zwischen den beiden in MCNPX-PoliMi implementierten Optionen hin.

---

<sup>1</sup>Berichtigung nach Druck: Wie in Abschnitt 3.1 beschrieben, wurde dies durch Enrico Padovani (Polytechnic of Milan) bestätigt, pers. comm., 26.08.2013.



## Abstract

Neutron multiplicity counting is a powerful technique used to determine the mass of nuclear material. It requires accurate knowledge on the fission neutron multiplicity distribution. This study summarizes the understanding of the physical background of neutron multiplicities and investigates the implementation in MCNPX-PoliMi. In particular, different approaches to include the incident particle energy are compared.

To explain why neutrons are emitted from fission fragments, Weisskopf's evaporation theory is revisited. It determines the emission probability as a function of the fragment excitation energy. With some additions it can be shown that a Maxwellian energy distribution for the neutrons in the centre of mass system is predicted. Calculations by Leachman are presented, who uses empirical data to compute the excitations and applies results of the evaporation theory to determine the multiplicity distributions.

By using only two assumptions, Terrell shows that the multiplicities can be approximated by a Gaussian function. This is the first of two options to simulate neutron multiplicities in MCNPX-PoliMi. The second option is assumed<sup>2</sup> to be given by Zucker and Holden's evaluation of an experiment for  $^{235}\text{U}$ ,  $^{238}\text{U}$  and  $^{239}\text{Pu}$  with incident neutron energies between 0 and 10 MeV.

Finally, a quantitative description of the deviations between the multiplicity distributions predicted by Terrell and those by Zucker and Holden is developed for a simplified system. The results of this study indicate deviations between both options implemented in MCNPX-PoliMi.

---

<sup>2</sup>Note Added in Proof: This was confirmed by Enrico Padovani (Polytechnic of Milan) and the implementation is described in Section 3.1, pers. comm., 26.08.2013.



# Contents

<b>1. Introduction</b>	<b>1</b>
<b>2. Theory</b>	<b>3</b>
2.1. Origin of Nuclear Fission . . . . .	3
2.2. Bohr's Independence Hypotheses . . . . .	7
2.3. Fission Cross Sections . . . . .	8
2.4. Evaporation Theory and the Neutron Energy Spectrum . . . . .	13
2.4.1. The Weisskopf Spectrum . . . . .	13
2.4.2. Corrections to Weisskopf's Spectrum and Other Approaches . . . . .	17
2.5. Multiplicity Distribution . . . . .	20
<b>3. Implementation in MCNPX-PoliMi</b>	<b>25</b>
3.1. Neutron Multiplicities . . . . .	25
3.2. Energy Dependence of Neutron-Induced Fission Multiplicities for Fast Neutrons .	26
3.3. Neutron Energy Distribution . . . . .	32
<b>4. Conclusions</b>	<b>37</b>
<b>Acknowledgments</b>	<b>39</b>
<b>Bibliography</b>	<b>41</b>
<b>A. Re-Evaluation of Spontaneous Neutron Multiplicities</b>	<b>49</b>
<b>B. Supplementary Data on the Energy Dependence of <math>P(\nu)</math></b>	<b>51</b>



# 1

## Chapter 1.

---

# Introduction

The measurement of correlated neutrons from nuclear fission is a widely used and well established practise in the study of nuclear materials [1]. In spontaneous and neutron-induced fission between zero and about six neutrons can be created (higher numbers are considerably less probable). The distribution of their numbers is called the fission neutron multiplicity and can be used to determine the amount of nuclear material present in a sample. This has made the study of neutron multiplicities very important to the field of nuclear Safeguards and in particular also, for the possible future verification of nuclear weapons disarmament.

Though nuclear weapon arsenals have fallen significantly since their peak during Cold War, today there are still more than 17.000 warhead in the inventories of the nine de-facto nuclear weapon states [2]. In order to pursue substantially deeper cuts it is widely considered helpful to conduct verification measures on warhead dismantlement. A key task in such a verification scenario is to ensure that the item subject to disarmament is a real nuclear warhead and not a mock-up. The exact specifications on nuclear warhead designs are confidential; however, in order to be able to lead to a nuclear explosion, several physical boundaries can be defined as attributes of a warhead. For instance there needs to be a minimum mass of nuclear material present so that a chain-reaction can be initiated. Since a chain-reaction should not be initiated accidentally, the amount of spontaneously fissioning isotopes have to be reduced. Thus the total mass is provided mainly by so called fissile isotopes, which have low spontaneous fission yields, but are readily fissionable by (low energy) neutrons. Applying the two criteria for example to a modern plutonium based nuclear weapon this means that one has to verify the presence of more than 500g plutonium in the warhead with an isotopic composition of less then 10%  $^{240}\text{Pu}$  (that has high spontaneous fission rates) and more then 90% of the fissile isotope  $^{239}\text{Pu}$  [3, Table 1].

In principal there are three types of radiation emitted from nuclear material,  $\alpha$ -particles,  $\gamma$ -particles and neutrons. The measurement of  $\gamma$ -radiation can be used to determine the isotopic composition. However, due to attenuation within a sample,  $\gamma$ -particles are not suitable to analyse the mass – a significant amount of the radiation from inside the sample does can be able to escape it and thus does not contribute to the measurement. The same holds true for an  $\alpha$ -particle which can be absorbed by singular nucleus under emission of one neutron in an  $(\alpha, n)$ -reaction.

Neutron detection may in general be used to find the sample mass, but the situation here is more complex. In passive neutron counting, the neutron count rate depends on the detection efficiency (known from calibrations) and three major unknowns: the spontaneous fission rate of the sample (proportional to the mass), the  $(\alpha, n)$ -reaction rate and the sample self-multiplication

[4]. This multiplication describes how many neutrons are created by induced fission in addition to those directly resulting from spontaneous fission. For the measurements it is made use of the fact that  $(\alpha, n)$ -reactions produce only one neutron per event, where as in spontaneous and induced fission up to six and more neutrons are (almost) simultaneously created. Thus discrimination between these neutron sources can be achieved by measurement of the temporal correlation between detected neutrons. The principle of neutron multiplicity measurements is, in addition to the total count rate and the correlation, to obtain a third parameter, closely connected to the multiplicity distribution [4]. Then the mass of spontaneously fissioning material in the sample can be calculated. If the isotopic ratio is known from  $\gamma$ -detection it is further possible to determine the mass of  $^{239}\text{Pu}$  present.

Since the emission of neutrons is of statistical nature, for a single event one can not know how many particles are created, based on many events the probability for the creation of a certain neutron number can be determined. These probabilities are calculated by knowledge of the physical background and empirical data. It is then even possible to simulate a measurement. Simply said, the computer takes the roll of “throwing the dice” and counts how many neutrons are emitted and how many arrive at the detector. A widely distributed computer code used in nuclear physics is the **Monte Carlo N-Particle** code MCNP, which can simulate the transport and reactions of neutrons, gammas and electrons [5]. Earlier version made incorrect physical assumptions on the multiplicity distributions, there have been several modifications to the code since then. The first major improvement concerning the implementation of fission multiplicities is included in MCNP-DSP, which samples from the full multiplicity distribution. Recently, with the development of MCNPX-PoliMi, it is attempted to add a correlation between the number and energy of emitted neutrons [6].

The first chapter of this study reviews the theory of the fission and neutron emission. In analogy to thermodynamic processes, the discharge of a neutron from a fission fragment is regarded as the particle’s evaporation from the nucleon. The associated emission probability is derived. Finally, two of the earliest and still most widely used approaches to describe the fission neutron multiplicities are presented.

The second chapter focuses on the models and empirical data underlying the simulation of neutron multiplicities in MCNPX-PoliMi. It analyses how the probabilities for neutron emission and the associated energies are implemented. Finally, it also compares different implementations for the induced fission neutron multiplicities with a particular focus on their dependence on the incident neutron energy.

# 2 Chapter 2.

---

## Theory

### 2.1. Origin of Nuclear Fission

One of the earliest and most intuitive models to facilitate the understanding of nuclear fission compares the nucleus with a liquid drop. The idea was first proposed by Gamow in 1929 for the atomic nucleus [7] and subsequently further developed by Carl Friedrich von Weizsäcker deriving the semi-empirical mass Equation [8]; with Bethe and Bacher's inclusion of the pairing energy it also became known as the Bethe-Weizsäcker mass formula [9]. After the discovery of nuclear fission Bohr and Wheeler, in 1939, elaborated this in their paper "The Mechanism of Nuclear Fission" on the basis of the liquid drop model [10].

In the basic concept of the liquid drop model the total binding energy is derived by a comparison of attractive strong nuclear forces between all nuclei and repulsive electrostatic interaction of the protons only. For the short range of the strong nuclear forces the influence of any other nucleons but the nearest-neighbours is considered negligible. Moreover, in the theoretical model these forces can be approximated by considering volume and surface size of the droplet (presuming a known size of its constituents, the nucleons). The volume term hereby refers to interactions within the droplet and should be proportional to number of nucleons inside it,  $A$ ; however, some corrections need to be applied as the particles on the droplet surface have fewer nearest neighbours and therefore, are bound less. The surface particles' net attraction towards the centre of the droplet results in surface-tension-like effects which are also responsible for the spherical shape in the ground state. The surface term of a sphere proportional to  $A$  nucleons therefore has the dependency on  $A^{2/3}$ .

The repulsive forces are given through the interaction amongst protons and as the Coulomb force has a much wider range, the number of protons  $Z$  present has to be included. The energetic contribution to the binding energy of the Coulomb force  $E_C$  is given by  $E_C \propto -Z_1 Z_2 / r$ , where each proton is repelled by all other protons (but itself) so that  $Z_1 Z_2 = Z(Z - 1)$ . For large  $Z$  this can be approximated by  $Z^2$ . The radius  $r$  of the droplet is derived from same considerations as above so that  $r \propto A^{1/3}$ . [11]

The three effects named above, the volume, surface and Coulomb terms already reproduce the general trend of the binding energies. However for heavier nuclides they overestimate the binding energy. This is improved by the introduction of the so called symmetry term of the form  $-(A - 2Z)^2 / A$ , and can be derived from quantum mechanical considerations in the Thomas-Fermi model [12]. At last the pairing term  $\delta(A, Z)$  was introduced by Bethe and Bacher to account for total energy minimization when the spins of each pair of protons or neutrons can couple. Pairing

therefore gives an explanation why isotopes consisting of even-even nucleon numbers are more stable than those with odd-odd numbered nucleons [9]. The pairing energy is mass dependent, as the nucleon wave functions in larger nuclides have a smaller overlap, thus resulting in a decreased coupling<sup>1</sup> [13, p.21].

The Bethe-Weizsäcker formula for the total binding energy  $E_{B,tot}(Z, A)$  is finally given by the sum of all terms above, each with an empiric coefficient  $k_i$  that is determined by a fit to experimental data:

$$E_{B,tot}(Z, A) = k_v A - k_{sur} A^{2/3} - k_c \frac{Z(Z-1)}{A^{1/3}} - k_{sym} \frac{(A-2Z)^2}{A} \pm \frac{\delta'}{A^{1/2}}; \quad k > 0. \quad (2.1)$$

$$\begin{aligned} k_v &= 15.5 \text{ MeV} & k_{sur} &= 16.8 \text{ MeV} \\ k_c &= 0.715 \text{ MeV} & k_{sym} &= 23 \text{ MeV} \\ \delta' &= 11.3 \text{ MeV} \end{aligned}$$

Table 2.1.: Constants used in the mass formula (2.1) from [12, p.52]. The uncertainty was not quoted.

The mass of a nucleus can be calculated if the binding energy is known. If its mass exceeds the sum of the fragment masses into which it could be divided, the nucleus is unstable against fission. Historically the first and most important model for the nuclear fission process used the liquid drop analogy. It was explored by Meitner [14], Bohr and Kalckar [15] and subsequently given a more detailed theoretical foundation by Bohr and Wheeler [10]. They suggested that “modes of motion of the nuclear matter similar to the oscillations of a fluid under the influence of surface tension” are to be expected due to the excitation energy of a nucleus. It gives rise to the possibility of small deformations, which can cause transformation to droplets only connected by a narrow neck; this is the so called saddle-point configuration. From the saddle point the two droplets may form (scission into) two separate fragments – This is the very origin of nuclear fission (see Fig. 2.1). One should note however, that for the short time-scales and lack of possibilities to directly observe the process, the exact mechanism of the nuclear fission is a highly difficult and long debated issue<sup>2</sup>.

Bohr and Wheeler investigated *inter alia* the influence of the nuclear charge  $Z$  on the fission probability for various deformations. From the Bethe-Weizsäcker formula (2.1) it can be calculated, that any deformation from the spherical ground state will at least initially require additional energy. However, Bohr et al. concluded that a higher relative nuclear charge ( $Z^2/A$ ) increases the scission probability as it effectively counteracts surface-tension like forces that would restore the original spherical shape. Upon reaching a critical value, even infinitesimal deformations will result in an unstable configuration. For isotopes with smaller charge, the potential energy associated with the deformation at the saddle point, which can be defined as the height

<sup>1</sup>With different assumptions one calculates a mass dependence proportional to either  $A^{-1/2}$  or  $A^{-3/4}$  [9, p.50].

For Equation (2.1) the first dependence was used in accordance with [11].

<sup>2</sup>One example of an issue where there is still no common interpretation is the explanation of asymmetric fission [16].

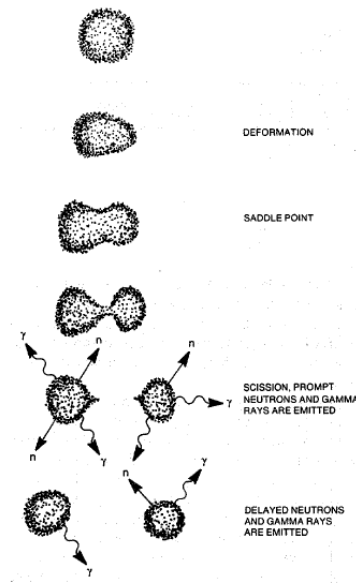


Figure 2.1.: Spontaneous fission of a nucleus in the liquid drop model. After deformation exceeding the saddle point, two separate droplets are formed. In less than  $10^{-3}$  sec, the excited fission fragments emit prompt neutrons and in less than  $10^{-14}$  to  $10^{-7}$  gammas follow as the fragment de-excites to lower energy levels [17]. Within a short time, the fragments may further undergo  $\beta^-$ -decay into other isotopes that can subsequently (within about  $10^{-1}$  to  $10^2$  sec)[17] emit delayed gammas or for some fragments also delayed neutrons. Reproduced from [18, p.338]

of the fission barrier<sup>3</sup>  $E_f$ , will be the decisive factor for the fission probability. A sketch of the fission process is shown in Figure 2.2.

In the classical picture fission would be impossible, if the total excitation energy  $E^*$  of the nucleus does not exceed the fission barrier  $E_f$ . Yet, quantum-mechanical tunnelling enables the nucleus to scission into fragments though it possesses less energy  $E^*$  than the fission barrier  $E_f$ . In fact it might even be in the ground state, which is the case for spontaneous fission. The height of the fission barrier was calculated by Frankel and Metropolis [19] with the addition of the pairing term by Vandenbosch and Seaborg [20]

$$E_f = 19\text{MeV} - 0,36\text{MeV} \frac{Z^2}{A} + \delta_{fiss}, \quad (2.2)$$

where the pairing term  $\delta_{fiss}$  is zero for even-even, 0.4 MeV for even-odd and 0.7 MeV for other nuclei.

Bohr and Wheeler [10] calculated an approximate “mean lifetime against fission in the ground state”  $t_{1/2, sf}$  for  $^{239}\text{Pu}$  of  $10^{22}$  years, which is much larger than the lifetime against  $\alpha$ -decay<sup>4</sup>. For elements with a higher nuclear charge  $Z$ , like californium, the fission probability can be in

<sup>3</sup>More precisely, one can imagine different shapes of transition sequences that result in the formation of two separate fragments. The energy of interest is the minimum value of the barrier height at saddle point for all possible transitions.

<sup>4</sup>Although current evaluations show that  $t_{1/2, sf} = (8. \pm 2.) \times 10^{15} \text{a}$  [21], where as the over all half-life is  $t_{1/2} = (24.11 \pm 0.03) \times 10^3 \text{a}$  (and the branching ratio for spontaneous fission is much smaller than 1%) [22].

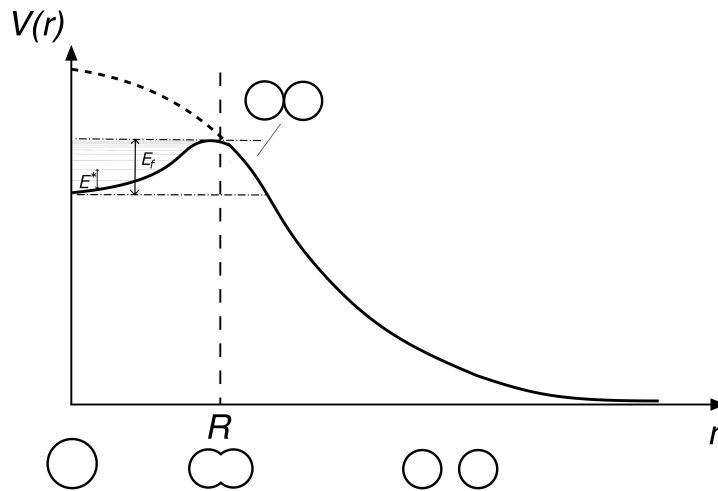


Figure 2.2.: The fission barrier. The Figure shown a continuous lines for the potential energy of the fissioning nuclide at different phases and depicts the corresponding shape in the liquid drop model. The difference between the height of the fission barrier  $E_f$  and excitation energy  $E^*$  determines the fission probability. The dashed line represents the potential for  $Z^2/A \geq 48$  where the fission barrier vanishes. Adapted from [13, edited].

the order of the  $\alpha$ -decay rate [18, p.338]. Due to nuclear spin effects like  $\delta_{fiss}$  in eq. (2.2)[23], a large decrease in the fission rates is observed for odd-even (about  $10^{-3}$ ) and odd-odd isotopes ( $10^{-5}$ ) in comparison to the even-even isotopes [18, p.338].

There is a second mechanism leading to fission which describes the bombardment of the isotope  $(A, Z)$  with neutrons. Those isotopes with at least one odd nucleon number are readily fissionable by the induced fission. It can easily be understood as a two fold process, first the absorption of the incident neutron under formation of a compound nucleus  $C$  with  $(A + 1, Z)$  and second the disintegration in one of the competing channels. In general the two possible channels are the de-excitation by gamma emission (hence this channel does not lead to fission) or the scission into two fragments as described above. For the latter process the energetic difference to spontaneous fission rises due to the fact that, in addition to the neutrons kinetic energy, the absorption releases the neutron binding energy of approximately 6 MeV. For isotopes with odd neutron and/or proton numbers, there is an additional release of the pairing energy  $\delta(A + 1, Z) \approx \delta'/\sqrt{240} \approx 0,72MeV$  that is subsequently available as excitation energy. The compound nucleus therefore has an excitation energy close to or above the fission barrier  $E_f$ . As an example this effect is observed for  $^{235}\text{U}$  and  $^{239}\text{Pu}$  which are readily fissionable even by neutrons with zero kinetic energy, whilst having small spontaneous fission yields [18, p.338].

Table 2.2 lists the fission barrier height  $E_f$  and excitation  $E^*$  of several isotopes for slow neutron bombardment. For  $E^* - E_f > 0$  induced fission with slow neutrons should be allowed,

for  $E^* - E_f < 0$  it is only possible by tunnelling. The excitation energy  $E^*$  is calculated using Equation (2.1) for zero kinetic energy neutrons

$$\begin{aligned}
 E^* &= m(A+1, Z) - m_n - m(A, Z) \\
 &= ((A+1) - Z)m_n + Zm_p - B(A+1, Z) - m_n - (A-Z)m_n + Zm_p - B(A, Z) \\
 &\stackrel{Taylor}{\approx} k_v - \frac{2}{3}k_{sur} \frac{1}{A^{1/3}} + \frac{1}{3}k_c \frac{Z(Z-1)}{A^{4/3}} - k_{sym} \left( 1 - \left( \frac{2Z}{A} \right)^2 \right) \pm \frac{\delta'}{A^{1/2}}, \tag{2.3}
 \end{aligned}$$

where the  $m_p$  is the proton mass and the Taylor expansion was approximated with an infinite target mass.

Table 2.2.: Excitation energy  $E^*$  of the compound nucleus formed by slow incident neutron bombardement compared with the fission barrier  $E_f$ .

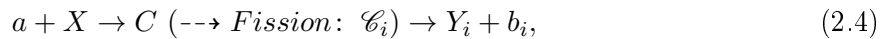
$Z$	$A$	$A+1$	Excitation $E^*$ [MeV]	Fission Barrier $E_f$ [MeV]	$E^* - E_f$ [MeV]
92	$^{235}\text{U}$	$^{236}\text{U}$	6.77	6.09	0.68
92	$^{238}\text{U}$	$^{239}\text{U}$	5.67	6.65	-0.98
94	$^{239}\text{Pu}$	$^{240}\text{Pu}$	6.94	5.75	1.19
94	$^{240}\text{Pu}$	$^{241}\text{Pu}$	5.36	6.2	-0.115

## 2.2. Bohr's Independence Hypotheses

The idea of the compound nucleus formation mentioned above are based on Bohr's independence hypothesis. In an address delivered before the Copenhagen Academy in 1936 Bohr presented the core idea as follows:

The phenomena of neutron capture thus force us to assume that a collision between a high speed neutron and a heavy nucleus will in the first place result in the formation of a compound system of remarkable stability. The possible later breaking up of this intermediate system by the ejection of a material particle or its passing with emission of radiation to a stable final state must in fact be considered as separate competing processes which have no immediate connection with the first stage of the encounter. [24, p.344]

We can then depict a nuclear reaction involving the compound nucleus  $C$  as



where  $a$  is the incident particle (in our case a neutron) and  $X$  is the target (here uranium or plutonium). The compound nucleus  $C$  subsequently emits a particles (neutron or gamma)  $b$  and leaves the residual nucleus  $Y$ . If  $C$  fissions, the fragments  $\mathcal{C}_i$  are created which may de-excite under the emission of particles  $b_i$  to leave the residual nuclei<sup>5</sup>  $Y_i$ . The two steps, formation and disintegration of the compound nucleus  $C$  (and  $\mathcal{C}_i$ ) can be regarded "as independent processes,

<sup>5</sup>Without loss of generality, only the simplest case with two fission fragments ( $i = 1, 2$ ) will be regarded here and later in the text.

in the sense that the mode of disintegration of the compound system depends only on its energy, angular momentum and parity, but not on the specific way in which it has been produced.” [25, p.340]

The hypothesis is based on the effect of strong but short-ranged nuclear interactions. From a comparison of the mean free path  $\Lambda$  of the incident particle with the target radius  $r_X$  one concludes that the exchange of the incident particle’s energy  $\epsilon_n$  among the whole nucleus  $X$  is much faster than the compound system could disintegrate. Thus, the state of the system at disintegration does not depend on the specific way of its formation. This argumentation, as well as the following calculations, are based on Blatt and Weisskopf [25, p.340f].

The mean free path  $\Lambda$  is defined as  $\Lambda = (\sigma\rho)^{-1}$ , where  $\sigma$  is the cross section for collisions with other nucleons and  $\rho$  is the nucleus density. An empirical value for the neutron-proton scattering cross section is given by Blatt and Weisskopf in *barns* as  $\sigma \approx (4\text{MeV}/E)$  for a relative kinetic energy  $E > 10$  MeV. Now  $\rho$  can be expressed with the nuclear radius  $R$  and the empirical radius parameter  $r_0 \approx 1.5 \times 10^{-13}\text{cm}$  through

$$\rho = \frac{A}{4/3\pi R^3} = 3 \frac{A}{4\pi(r_0 A^{1/3})^3} = \frac{3}{4\pi r_0^3}. \quad (2.5)$$

The relative kinetic energy  $E$  used in the approximation of the cross section  $\sigma$  is  $E \approx 1/2(E_0 + \epsilon_n)$  with the average kinetic energy per nucleon  $E_0 = h^2/(8 \times 4 r_0^2 m_{\text{nucleon}}) \approx 20\text{MeV}$ . [10] Combining the above Equations we receive for the mean free path  $\Lambda$  the following relation, where  $\epsilon_n$  and  $E_0$  are expressed in MeV

$$\Lambda \approx 1.8 \times 10^{-15}(\epsilon_n + E_0) \text{ cm}. \quad (2.6)$$

So with an incident neutron energy of  $\epsilon_n = 20$  MeV we arrive at a mean free path  $\Lambda \approx 7 \times 10^{-14}$  that is much smaller than the nuclear radius  $r_0$ . Thus, once the nucleon is absorbed, it undergoes many collisions and its energy is quickly shared through its interaction with other nucleons. The energy is statistically distributed amongst all nuclei, for a large nucleus the energy will be approximately equal for all constituents. Blatt and Weisskopf conclude that the conditions for the hypothesis to be valid are that  $\Lambda \ll r_0$  and  $\epsilon_n \ll (A-1)E_B$ , where  $E_B$  is the binding energy of a single nucleon. Both conditions are met for  $A > 10$  and incident neutron energies  $\epsilon_n < 50$  MeV.<sup>6</sup>

For higher energies Bohr already correctly assumed that more than one particle could be emitted and “for still more violent impacts [...] we must even be prepared for the collision to lead to an explosion of the whole nucleus” [24, p.348].

### 2.3. Fission Cross Sections

Having explored Bohr’s independence hypothesis it is possible to explain the main characteristics of the neutron-induced fission cross section  $\sigma_{nf}$  as two independent processes. First the formation of a compound nucleus, which is the capture of a neutron, and second the disintegration of the compound system into fission products. The probability for the whole fission process will be a combination of the individual probabilities. The derivation below mainly follows Glasstone

<sup>6</sup>For a review of experimental tests of Bohr’s hypothesis see [26, p.108f].

and Edlund [27, p.25f].

In Figure 2.3 one observes a typical energy-dependent induced fission cross section spectrum for a heavy element. It can be divided into three main regions: the first before the resonances start (I), the resonance region from about 0.1 eV to 0.1 MeV (II) and higher energies where there are no resonances observable (III).

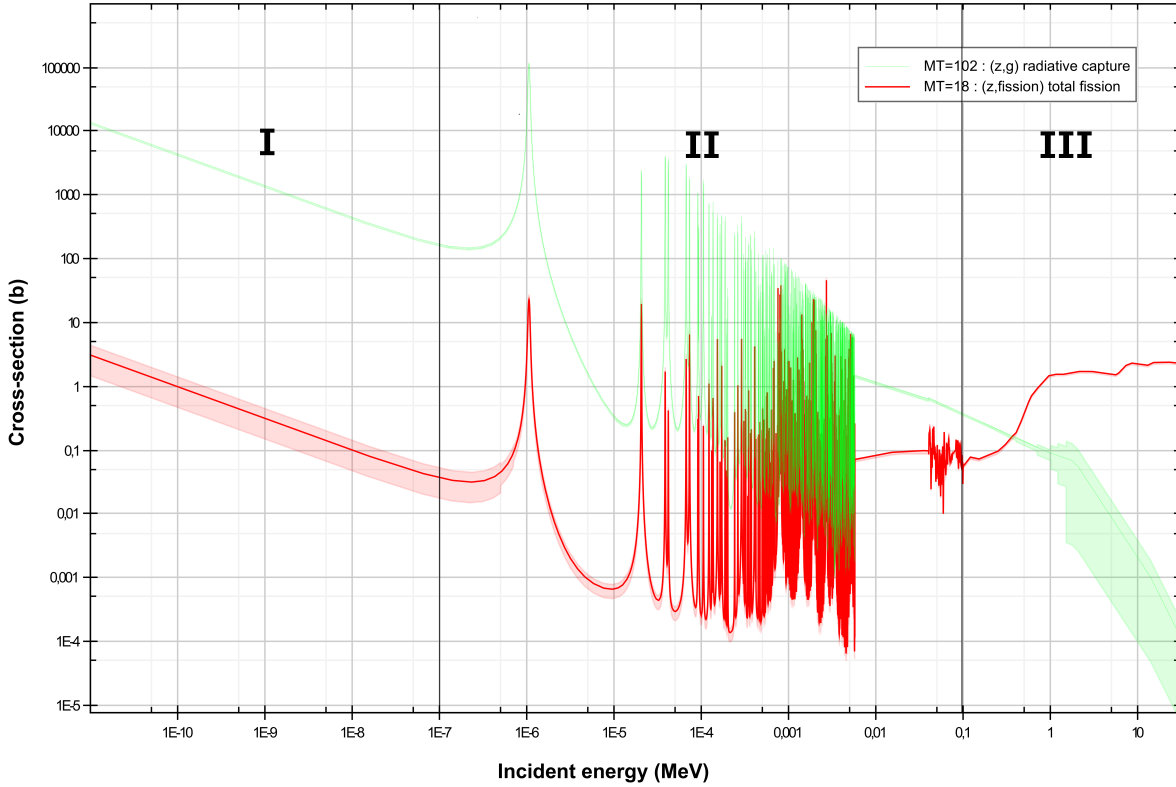


Figure 2.3.: Neutron-induced fission  $\sigma_{nf}$  (red) and radiative capture  $\sigma_{n\gamma}$  (green) cross sections for  $^{240}\text{Pu}$ ; the shaded area represents the uncertainty. One observes roughly three regions, the first before the resonances start (I), the resonance region from about 0.1 eV to 0.1 MeV (II) and the higher energy area where there are no resonances observable (III). [28]

The resonance behaviour dominates the cross section below about 0.1 MeV and originates from a highly increased neutron capture probability (also shown in Figure 2.3 for comparison). The latter arises as only neutrons with those energies  $\epsilon_n$  can be absorbed, that lead to the formation of an excited state which matches a quantum level  $E_r$  of the compound nucleus  $C$ . To be more precise, due to the natural broadening of  $E_r$ , the level formed with a neutron of energy  $\epsilon_n$  needs to be only close to  $E_r$ . This is visualized in Figure 2.4, where the lines to the right represent the quantum levels in the compound nucleus. In the middle there are hypothetical (target & neutron) levels, of which the first,  $E_0$  is for a zero kinetic energy neutron. It exceeds the ground state of  $C$  by the neutron binding energy.

In general  $E_0$  does not necessarily fall together with an existing quantum level of  $C$ , which makes  $E_1$  the first excitable state in this picture. Thus, the first resonance occurs at  $\epsilon_n = E_1 - E_0$ . Subsequent resonances will occur at those neutron energies leading to the formation of a quantum

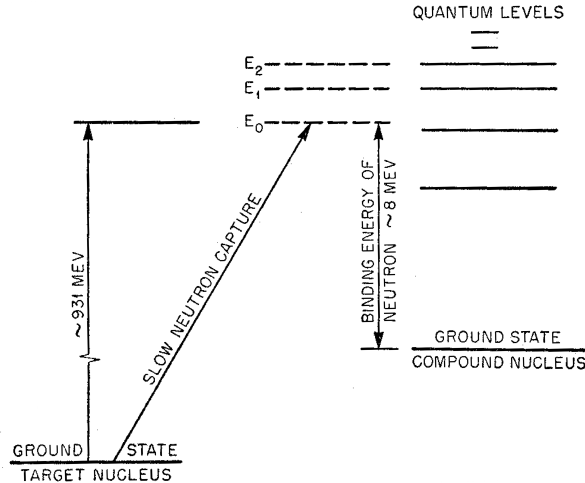


Figure 2.4.: Formation of compound nucleus  $C$  and energy levels. In the middle are several hypothetical levels of target & neutron, to the right are the actual quantum levels of  $C$  – only those can be realized. Reproduced from [27, p.25].

level of  $C$ , for instance  $E_2$ .

Applying the Schrödinger equation the absorption process, Breit and Wigner derived the following expression for the cross section at (one level) resonance between the levels  $g$  and  $e$

$$\sigma_{g \rightarrow e} = \frac{\lambda^2}{4\pi} \frac{\Gamma_a \Gamma_b}{(E - E_r)^2 + \frac{1}{4}\Gamma^2}, \quad (2.7)$$

where  $\Gamma_{a,b}$  are the levels widths of re-emission of the incident particle  $a$  and emission of outgoing particle  $b$ , respectively;  $\Gamma$  is their sum. For a particle,  $\lambda$  is the de Broglie wavelength. As used above,  $E_r$  is the energy that corresponds to an exact resonance with the specific level. For simplification only the one level formula is given here, which is valid only for sufficiently wide broadened levels.

To derive the cross section that only depends on the neutron energy  $\epsilon_n$ , we relate the level width  $\Gamma$  to the emission probability with the Einstein coefficient  $\mathcal{A}$  and the radiative lifetime  $\tau$  by Heisenberg's uncertainty relation  $\Gamma = \Delta E = \hbar/(2\tau) = \hbar/2 \mathcal{A}$ . Then, the assumption has to be made that  $\Gamma_b$ , corresponding to the emission probability of  $b$ , is independent of the formation process (so it is based on Bohr's hypothesis). In fact, this is the case at low energy states, as the neutron usually de-excites by gamma emission. In first approximation, only the gamma energy, not "the probability" and  $\Gamma_b$  vary with the incident neutron energy  $\epsilon_n$ . In contrast, the re-emission of the neutron for which the probability is represented by  $\Gamma_a$  can be shown to be proportional to its velocity, so  $\Gamma_a = \Gamma_n = \text{const.} \times \sqrt{\epsilon_n}$ . With a constant  $\alpha$  and the de Broglie wavelength<sup>7</sup>  $\lambda = h/p$  that is also proportional to  $1/\sqrt{\epsilon_n}$  Equation 2.7 now yields

$$\sigma_{nf} = \frac{\alpha}{\sqrt{\epsilon_n}} \frac{\Gamma_b}{(\epsilon_n - E_r)^2 + \frac{1}{4}\Gamma^2}. \quad (2.8)$$

The Breit-Wigner distribution is shown in Figure 2.5, where one obtains three regions.

<sup>7</sup>Actually calculating  $\lambda$  one should use the reduced mass, however for heavy targets ( $m_a \ll m_X$ ) is is approximately given by the mass of the projectile.

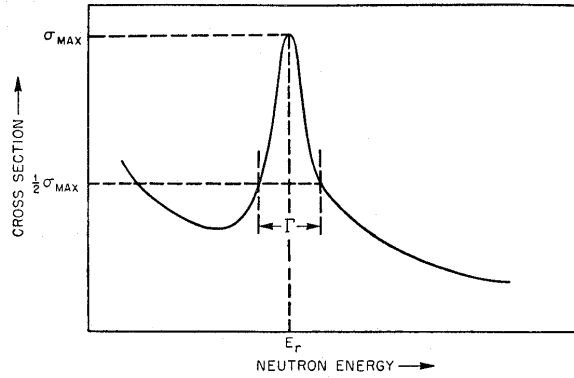


Figure 2.5.: Breit Wigner resonance peak for neutron capture at the resonance  $E_r$  with line width  $\Gamma$ . Reproduced from [27, p.29].

- Before (and after) the resonance,  $\epsilon_n \ll E_r$  ( $\epsilon_n \gg E_r$ ), one finds  $\sigma_{nf} \propto 1/\sqrt{\epsilon_n}$ . Therefore it is also called the “ $1/v$ -region”.
- Exactly at resonance  $E = E_r$  the cross section has its maximum

$$\sigma_{nf,\max} = \frac{A}{\sqrt{E_r}} \frac{4\Gamma_b}{\Gamma^2}. \quad (2.9)$$

when the one level Breit-Wigner formula is applied to each peak individually the expected behavior can be observed in Figure 2.3. At higher energies the resonance amplitude  $\sigma_{nf,\max}$  reduces, but interestingly the resonances also seem to overlap until they can not be resolved anymore<sup>8</sup>. This is a result of the increasing level density in the compound nucleus, thus decreased level spacing, which in a first approximation can be derived from a Fermi gas in a sphere (3-dim box.) where  $\rho \propto E^*$ .

The fission cross sections  $\sigma_{nf}$  of  $^{240}\text{Pu}$  given in Figure 2.3 exhibit the same characteristics as the capture cross section  $\sigma_{n\gamma}$  in region I and II. However  $\sigma_{nf}$ , which is a combination of the absorption and disintegration probability, is reduced between about  $10^4$  for lower and a factor of 10 for higher energies in comparison with  $\sigma_{n\gamma}$ . One concludes that the probability for the fission of the compound nucleus  $C$  must be very small at low neutron energies and increase for higher energies. This matches the result obtained in the fission barrier model, where the compound nucleus formed,  $^{241}\text{Pu}$ , as an even-odd nucleus has a lower excitation energy than the fission barrier; thus, fission only occurs by tunnelling through the barrier which in turn has a low probability.

At higher incident energies, the neutron provides enough energy for the compound nucleus deformation, and its excitation energy may even exceed the fission barrier. This is seen in region III, where the resonances overlap and vanish. However, when  $\epsilon_n$  gets sufficiently large to compensate the pairing effect, one sees a step-like increase in the fission cross section. The assumptions concerning  $\Gamma_a$  and  $\Gamma_b$  made for Equation (2.8) no longer hold true and for neutron energies above approximately 1 MeV any incident neutron will have enough energy to lead to

<sup>8</sup>Observe the double logarithmic scale. The resonances between about 0.05 and 0.1 MeV are not explained here due to the limited scope of the work. Interestingly, they were added only in the first (and currently latest) revision of the ENDF VII database.

fission. Thus the cross section approaches the geometrical value  $\sigma_{nf} = \pi R^2$ , where  $R$  is the nuclear radius. With the same parameter as in Equation (2.5), one finds

$$\sigma_{nf} = \pi R^2 = \pi * (r_0 * A^{1/3})^2 \approx 2.7b, \quad \epsilon_n \gg E_f, \quad (2.10)$$

where the last approximation is based on a nuclear mass of  $A = 240$ . The fission cross sections of fissile nuclei, like  $^{235}\text{U}$  and  $^{239}\text{Pu}$ , follow a very similar characteristic which is shown in Figure 2.6. The main difference is that due to the different pairing energy (for odd-even nuclei) the neutron does not need to provide kinetic energy to overcome the fission barrier. In contrary, according to Equation (2.8) with higher velocity the capture probability decreases. Therefore it is even more likely for fissile materials to fission at low neutron energies.

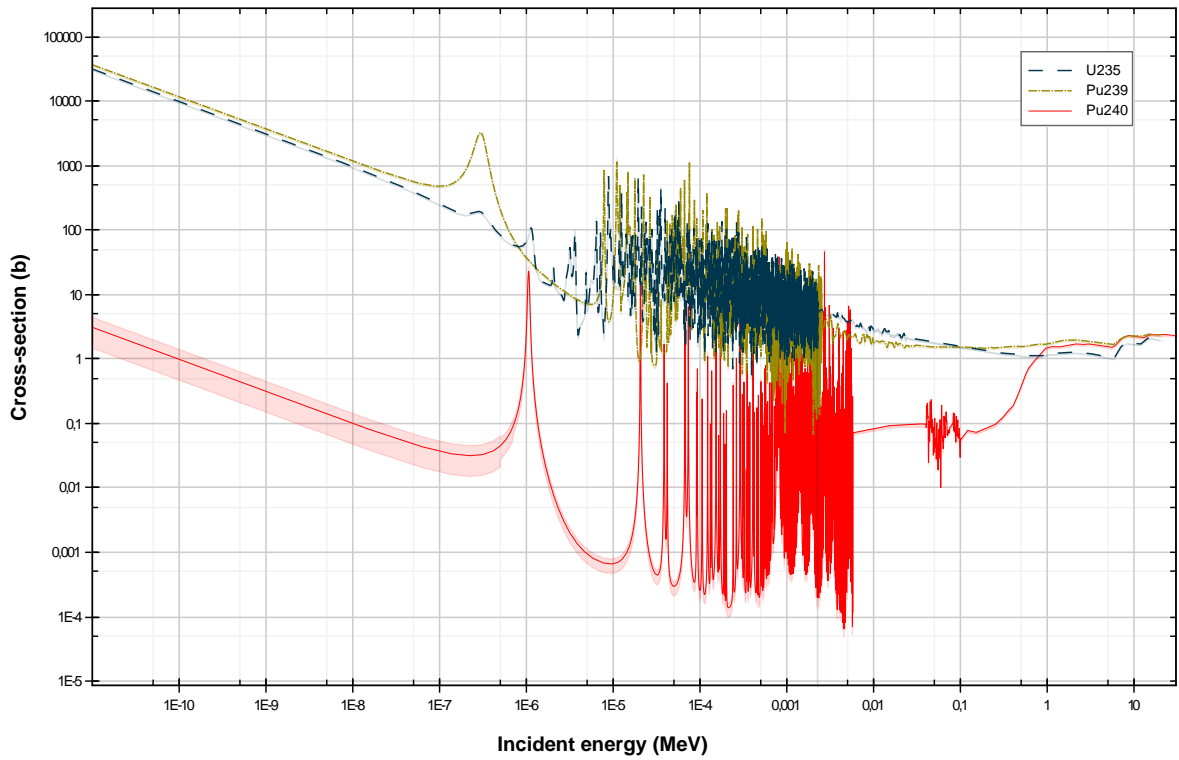


Figure 2.6.

Figure 2.7.: Neutron-induced fission cross sections of  $^{235}\text{U}$  (blue dashed),  $^{239}\text{Pu}$  (brown dotted) and  $^{240}\text{Pu}$ . The shaded area represents the uncertainty. [28–30]

## 2.4. Evaporation Theory and the Neutron Energy Spectrum

### 2.4.1. The Weisskopf Spectrum

In order to calculate the energy spectrum of neutrons emitted from fission fragments Weisskopf's statistical theory is followed. As first proposed by Frenkel [31], it compares the de-excitation process with the loss of heat energy by the removal of particles: Thus it is called evaporation theory. The derivation is based on Bohr's independence hypothesis and if not stated otherwise taken from Cole [26, p.111ff], who explains the physical picture involved in Weisskopf's original paper [32].

According to Bohr's independence theory it is equivalent to observe the disintegration or formation of a compound nucleus  $C$ . This statement also holds true for the compound  $\mathcal{C}$  resulting from scission of  $C$ , which may de-excite under the emission of particle  $b$  to leave the residual nucleus  $Y$ . The goal will be to find the probability per unit time  $W_n(\epsilon_n)d\epsilon_n$  for emission of the neutron  $n$  (more generally particle  $b$ ) with kinetic energy in the centre of mass system (CMS) between  $\epsilon_n$  and  $\epsilon_n + d\epsilon_n$ , hence transforming  $\mathcal{C}$  (with the excitation energy  $E_{\mathcal{C}}^*$ ) into the residual nucleus  $Y$ .

For the derivation following setting will be regarded: Some time  $\Delta t$  after the emission of the neutron  $n$  ejected from  $\mathcal{C}$ ,  $n$  is located within an arbitrary volume  $V$ , that is centred around the residual nucleus  $Y$ . In a good approximation for heavy nuclei,  $Y$  has zero velocity in the CMS and without loss of generality the volume  $V$  is of spherical shape. To gain statistical information it is then important that there are many possible reactions which differ in the energy of the emitted particle  $\epsilon_b$  and the excitation levels of  $\mathcal{C}$  and  $Y$  respectively. By the excitation energies one can define the number of microstates of the "decaying compound nucleus"  $\Omega_{\mathcal{C} \rightarrow nY}(\Delta t)$  that will be in direct correspondence to the "decayed states" ( $n + Y$ ) produced in  $V$ , for which the shorthand  $nY$  is used. Thus  $\Omega_{\mathcal{C} \rightarrow nY}(\Delta t)$  also represents the states in which the neutron  $n$  and the residual nucleus  $Y$  can be found inside  $V$ . In equilibrium, we can express the decay rate  $W_n(\epsilon_n)$  under emission of a neutron by the ratio of states decaying into ( $n + Y$ ) to all possible states  $\Omega_{\mathcal{C}}(E_{\mathcal{C}}^*)$

$$\Delta t W_n(\epsilon_n) = \frac{\Omega_{\mathcal{C} \rightarrow nY}(\Delta t)}{\Omega_{\mathcal{C}}(E_{\mathcal{C}}^*)} = \frac{\rho_{\mathcal{C} \rightarrow nY}(\Delta t)}{\rho_{\mathcal{C}}(E_{\mathcal{C}}^*)}. \quad (2.11)$$

In the above equation it was assumed that there are so many energy levels in the excited and residual nucleus, that the number of microstates  $\Omega$  can be represented by the continuous level densities  $\rho$ . For the further calculation it is useful to define the combined density of states  $\rho_{nY}$  for  $n$  and  $Y$  in the volume  $V$ , which is a convolution of the single particle densities. Next one multiplies eq. (2.11) by unity ( $\rho_{nY}/\rho_{nY}$ ) and arrives at

$$W_n(\epsilon_n) = \frac{1}{\Delta t \rho_{\mathcal{C}}(E_{\mathcal{C}}^*)} \frac{\rho_{\mathcal{C} \rightarrow nY}(\Delta t)}{\rho_{nY}} \rho_{nY}. \quad (2.12)$$

One finds that the ratio  $\rho_{\mathcal{C} \rightarrow nY}(\Delta t)/\rho_{nY}$  is the probability for states of  $\rho_{nY}$  to result from the compound system's decay. However this ratio can equivalently ("reversing the direction of trajectories") be identified as all those states in  $\rho_{nY}$  that will form the compound system  $\mathcal{C}$  within the time  $\Delta t$ .

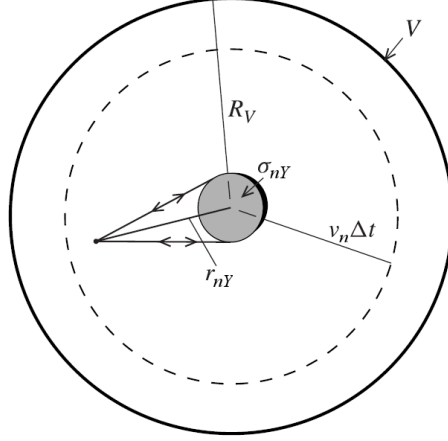


Figure 2.8.: Neutron evaporation in the Weisskopf picture. “Only those trajectories contained in the solid angle subtended by the cross-section  $[\sigma_{nY}]$ ” represent states of  $n$  and  $Y$  that will result in the formation of a compound nucleus  $\mathcal{C}$ . The distance between the neutron and the residual nucleus is given by  $r_{nY}$ ,  $v_n$  is the speed of the neutron, and  $R_V$  represents the radius of the volume  $V$  centred around the residual nucleus. Adapted from [26, p.133].

Next, in this reversed picture, one analyses the particular influence on the decay probability of the fraction of microstates  $\rho_{nY}$ , for which  $n$  has an absolute velocity<sup>9</sup> between  $(v_n, v_n + dv_n)$  and that lead to the formation of a compound nucleus  $\mathcal{C}$  within  $\Delta t$ . If  $\sigma_{nY \rightarrow \mathcal{C}} (= \sigma_{nY})$  is the cross-section for the reaction  $n + Y \rightarrow \mathcal{C}$ , then only those neutrons  $n$  that intercept  $\sigma_{nY}$  within  $\Delta t$  contribute to the formation of  $\mathcal{C}$ . As visualized in Figure 2.8, for a fix distance  $r_{nY}$  of  $n$  from  $Y$ , this contributing fraction of neutrons is given relative to the total solid angle  $4\pi$  by

$$q(r_{nY}) = \frac{\sigma_{nY}}{4\pi r_{nY}^2}. \quad (2.13)$$

To find all relevant microstates one has to average  $q(r_{nY})$  over all possible distances. It is first seen that there is no reaction for  $r_{nY}$  larger than  $v_n \Delta t$ , so  $q(r_{nY}) = 0$  for  $r_{nY} > v_n \Delta t$ . The lower bound of the integration can be set to  $r_{nY} = 0$ , introducing only a very small error for volumes  $V$  (which has the radius  $R_V$ ) much larger than the nucleus  $Y$ ,  $V \gg \sigma_{nY}$ . The average  $\langle q \rangle$  then yields

$$\begin{aligned} \langle q \rangle &= \frac{1}{V} \int_V q(r_{nY}) dV = \frac{1}{V} \int_{r_{nY}=0}^{R_V} q(r_{nY}) 4\pi r_{nY} dr_{nY} \\ &= \frac{1}{V} \int_0^{v_n \Delta t} \frac{\sigma_{nY}}{4\pi r_{nY}^2} 4\pi r_{nY} dr_{nY} = \frac{\sigma_{nY} v_n \Delta t}{V}, \end{aligned} \quad (2.14)$$

which is subsequently identified with the transition probability during the time  $\Delta t$  of either the states  $(n + Y)$  to form the compound system  $\mathcal{C}$ , or reversed, the decay of  $\mathcal{C}$  into  $(n + Y)$

<sup>9</sup>The velocity interval is easily connected to the energy interval by  $v_n = (2\epsilon_n/m)^{1/2}$

$$\frac{\rho_{\mathcal{C} \rightarrow nY}(\Delta t)}{\rho_{nY}} = \frac{\rho_{nY \rightarrow \mathcal{C}}(\Delta t)}{\rho_{nY}} = \frac{\sigma_{nY} v_n \Delta t}{V}. \quad (2.15)$$

Combining Equations 2.12 and 2.15, the contribution to the transition rate by particles with the velocity  $(v_n, v_n + dv_n)$  is

$$\begin{aligned} \frac{dW_{\mathcal{C} \rightarrow nY}}{dv_n} dv_n &= \frac{\sigma_{nY} v_n}{V} \frac{1}{\rho_{\mathcal{C}}(E_{\mathcal{C}}^*)} \frac{d\rho_{nY}}{dv_n} dv_n \\ &= \frac{dW_{\mathcal{C} \rightarrow nY}}{d\epsilon_n} d\epsilon_n = \frac{\sigma_{nY}}{V} \left( \frac{2\epsilon_n}{m_b} \right)^{1/2} \frac{1}{\rho_{\mathcal{C}}(E_{\mathcal{C}}^*)} \frac{d\rho_{nY}}{d\epsilon_n} d\epsilon_n. \end{aligned} \quad (2.16)$$

Next one calculates the energy dependence of  $\rho_{nY}$ . It is, as mentioned above, a convolution of the single particle densities for the neutron  $n$  and the residual nucleus  $Y$ , which has the excitation energy  $E_Y^*$ . For a single particle without internal excitation levels the number of states is simply

$$\Omega_n(\epsilon_n) = (2s + 1)V * V_p = (2s + 1)V * \frac{\frac{4}{3}\pi p^3}{(2\pi\hbar)^3} = (2s + 1)V * \frac{\frac{4}{3}\pi(2m_n\epsilon_n)^{3/2}}{h^3}, \quad (2.17)$$

where the spin-multiplicity  $2s + 1$ , impulse  $p$ , the volume in phase space  $V_p$  and the relation  $E_{kin} = \frac{p^2}{2m}$  were used. For the neutron which has spin  $s = 1/2$  the single particle density is given by

$$\rho_n(\epsilon_n) = \frac{d\Omega_n}{d\epsilon_n} = 2V \frac{2\pi(2m_n)^{3/2}\epsilon_n^{1/2}}{h^3} = \frac{8\pi V(2m_n)^{3/2}\epsilon_n^{1/2}}{h^3}. \quad (2.18)$$

The convolution integral of the combined micro state density  $\rho_{nY}(E_{nY})$  for the system  $n + Y$  with the total energy  $E_{nY} = \epsilon_n + E_Y^* = E_{\mathcal{C}}^* - E_B$  therefore yields in the interval  $(\epsilon_n, \epsilon_n + d\epsilon_n)$

$$\rho_{nY}(E_{nY}) = (\rho_n * \rho_Y)(E_{nY}) = \int_0^{E_{nY}} \rho_n(\epsilon_n) \rho_Y(E_{nY} - \epsilon_n) d\epsilon_n \quad (2.19)$$

$$\frac{d(\rho_{nY}(E_{nY}))}{d\epsilon_n} d\epsilon_n = \rho_n(\epsilon_n) \rho_Y(E_{nY} - \epsilon_n) d\epsilon_n = \frac{8\pi V(2m_n)^{3/2}\epsilon_n^{1/2}}{h^3} \rho_Y(E_{nY} - \epsilon_n) d\epsilon_n \quad (2.20)$$

Combining equation (2.16) and (2.20) one finally obtains Weisskopf's evaporation formula<sup>10</sup>, as the transition rate between  $\mathcal{C}$  and  $n + Y$  for the kinetic energy  $\epsilon_n$

$$\frac{dW_{\mathcal{C} \rightarrow nY}}{d\epsilon_n} d\epsilon_n = \sigma_{nY} \frac{16\pi m_n \rho_Y(E_{nY} - \epsilon_n)}{h^3 \rho_{\mathcal{C}}(E_{\mathcal{C}}^*)} \epsilon_n d\epsilon_n. \quad (2.21)$$

Furthermore Weisskopf introduced the microcanonical entropy to the system. Using the general definition<sup>11</sup>  $S(E) = \ln[\rho(E)]$ , Equation (2.21) can be rewritten, expressing the discharge of a particle with mass  $m$  from a system with the energy  $E_{\mathcal{C}}^*$  and entropy  $S_{\mathcal{C}}(E)$  and the residual nucleus' entropy  $S_Y(E)$

<sup>10</sup>Weisskopf derived it slightly more general for a particle  $b$  with spin  $s$  and as stated in [26, p.115] "he denoted by [Planck's constant] 'h' the symbol which is nowadays referred to as  $\hbar = h/2\pi$ ."

<sup>11</sup>Observe that the Boltzmann constant  $k_b$  is omitted in this definition, so that the nuclear temperature introduced in Equation (2.24) has the dimensions of an energy.

$$\frac{dW_{\mathcal{C} \rightarrow nY}}{d\epsilon_n} d\epsilon_n = \sigma_{nY} \frac{16\pi m_n}{h^3} e^{S_Y(E_{nY} - \epsilon_n) - S_{\mathcal{C}}(E_{\mathcal{C}}^*)} \epsilon_n d\epsilon_n. \quad (2.22)$$

From this formula with general validity, several simplifications can be made. From here on Weisskopf's original paper [32] is followed, as it contains more details on them.

To simplify the entropy terms, the first assumption states that the excitation energy  $E_{\mathcal{C}}^*$  is much larger than the neutron binding energy  $E_B$  and kinetic energy  $\epsilon_n$  ( $E_{\mathcal{C}}^* \gg E_B, E_{\mathcal{C}}^* \gg \epsilon_n$ ). Moreover the strong approximation is used, that the microstate densities of  $Y$  and  $\mathcal{C}$  are identical around the energy  $E_{nY}$  ( $S_{\mathcal{C}}(E) = S_Y(E)$ ), therefore the development in first order is

$$S_Y(E_{nY} - \epsilon_n) = S_Y(E_{\mathcal{C}}^* - E_B - \epsilon_n) = S_{\mathcal{C}}(E_{\mathcal{C}}^*) - (E_B + \epsilon_n) \left. \frac{dS_{\mathcal{C}}}{dE} \right|_{E_{\mathcal{C}}^*}. \quad (2.23)$$

The derivative of the entropy  $S_{\mathcal{C}}$  can be expressed by the nuclear temperature  $T_{\mathcal{C}}(E)$ , where  $E$  is the most probable energy of the nucleus  $\mathcal{C}$  in thermodynamical equilibrium.

$$\frac{dS_{\mathcal{C}}}{dE} = \frac{1}{T_{\mathcal{C}}(E)}. \quad (2.24)$$

Equation (2.22) can be rewritten with this definition as

$$\frac{dW_{\mathcal{C} \rightarrow nY}}{d\epsilon_n} d\epsilon_n = \sigma_{nY} \frac{16\pi m_n}{h^3} e^{-E_B/T_{\mathcal{C}}(E_{\mathcal{C}}^*)} \epsilon_n e^{-\epsilon_n/T_{\mathcal{C}}(E_{\mathcal{C}}^*)} d\epsilon_n, \quad (2.25)$$

which is exactly the formula for the classical thermodynamical evaporation.

The problem for the emission of particles is, that the assumptions established concerning  $E_{\mathcal{C}}^*$  and the entropies leading to Equation (2.25) are not fulfilled. For example the binding energy  $E_B$  of about 6 MeV is not much smaller than the excitation of the compound system  $E_{\mathcal{C}}^* \approx 10 \text{ MeV} = 1/2 * \bar{\nu}(E_B + \epsilon_n)$  (here approximated with the average neutron multiplicity  $\bar{\nu} \approx 2.5$  equally shared between two fragments and a neutron energy  $\epsilon_n = 1 \text{ MeV}$ ). Nevertheless Weisskopf finds a similar approximation as Equation (2.23) where he only assumes that the neutron kinetic energy,  $\epsilon_n$  is much smaller than the difference between the compound state excitation energy and the binding energy  $\epsilon_n \ll E_{\mathcal{C}}^* - E_B$ , which should be fulfilled at least for the initially evaporated neutrons. The nuclear temperature considered will then be temperature of the remaining nucleus  $T_Y(E)$ . Besides, higher order terms in eq. (2.25) have not been considered, however Weisskopf shows that this correction they small in comparison with the other terms appearing in the Equation.

The final expression for Weisskopf's emitted neutron spectrum is according to Equation (2.25) and the corrections in the paragraph above

$$W_n(\epsilon_n) d\epsilon_n = \frac{dW_{\mathcal{C} \rightarrow nY}}{d\epsilon_n} d\epsilon_n \approx \text{const.} \times \sigma_{nY} \epsilon_n e^{-\epsilon_n/T_Y(E_{\mathcal{C}}^* - E_B)} d\epsilon_n. \quad (2.26)$$

This spectrum<sup>12</sup> is of the same form as in equation (2.25), however the parameter is the nuclear temperature  $T_Y(E_{\mathcal{C}}^* - E_B)$  of the residual nucleus at its most probable energy, not of the compound system any more. Though not explicitly expressed in the above formulas, (especially for lower energies) one should bear in mind, that the cross section  $\sigma_{nY}$  is also energy-dependent.

<sup>12</sup>Weisskopf denoted it as a Maxwell distribution, for the proportionality to  $\epsilon_n \exp[-\epsilon_n/T(E)]$  represents the Maxwell probability density function. In order to avoid confusion with the Maxwell energy spectrum derived from the ideal gas model, this notation was not adopted. As it will be explained, the Maxwell energy spectrum is proportional to  $\sqrt{\epsilon_n} \exp[-\epsilon_n/T(E)]$ .

### 2.4.2. Corrections to Weisskopf's Spectrum and Other Approaches

On the application of Weisskopf's evaporation formula (2.26) to experimental data 1952 Watt noticed significant deviations [33]. Figure 2.9a shows a comparison of data acquired by Hill [34] and Watt himself with a modified Weisskopf spectrum; however, especially for energies higher  $\epsilon_n > 7$  MeV, no good fit could be achieved. The spectrum was modified based on Feather's assumption [35] which states that the actual observed spectrum should be a weighted sum over the evaporation spectra of all fission fragment pairs. As such computations were very laborious at that time, Watt approximated the sum by adding up the spectra of the average energy and mass of the light and heavy fragment group. The result can be seen in Figure 2.9b.

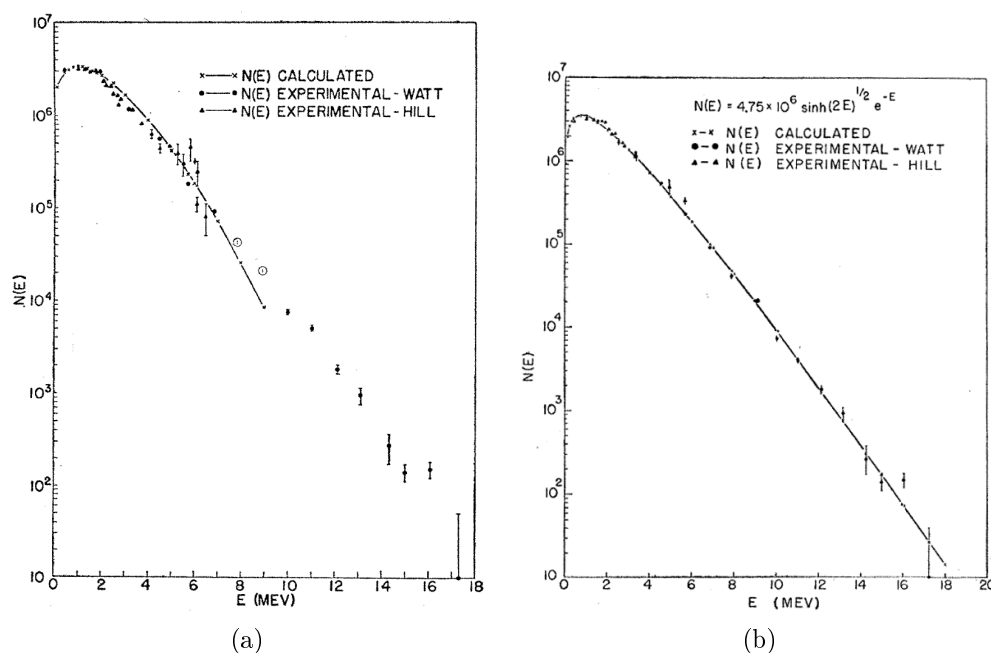


Figure 2.9.: Neutron energy spectrum from induced fission of U-235 in laboratory system. The calculated curve in (a) is a Weisskopf spectrum based on Feather's assumptions the two fission fragments. As can be seen, above about 7 MeV the calculations deviate significantly from the experiments. In (b) the Watt spectrum is shown, which obviously is in better agreement with the experimental data by Watt [33], Hill [34]. Adapted from [33].

Watt achieved a much better agreement by assuming a Maxwellian distribution of the neutron velocity in the centre of mass system instead of the Weisskopf evaporation formula. In the laboratory system the Maxwell velocity distribution yields the following formula for the neutron emission probability  $N(\epsilon_n)$  which has become known as the Watt spectrum<sup>13</sup>.

$$N(\epsilon_n) = const. \times e^{-\epsilon_n/T_W} \sinh \left[ 2 \frac{\sqrt{\epsilon_n \frac{m_n}{M} E_Y}}{T_W} \right], \quad (2.27)$$

<sup>13</sup>On the origin Watt states that "Several early reports on the fission spectrum mention this formula but none give the originator. It seems likely that it was derived by several investigators and spread by private communications." [33, p.1040]

where the temperature  $T_W$  is a fit-parameter,  $E_Y$  is the fission fragment kinetic energy at the time of neutron emission and  $m_n$  and  $M$  are the neutron and fragment masses. It is an empirical formula only and there is no real physical derivation. One could obtain it from the velocity distribution of an ideal gas in contact with a heat bath, where the momentum distribution is given by [26]

$$\frac{d\Omega(p)}{dp} dp = \frac{V}{h^3} e^{-p^2/(2mT)} 4\pi p^2 dp \quad (2.28)$$

Substituting  $\epsilon_n = p^2/2m$  it can be transformed to an energy distribution

$$\rho(\epsilon_n) d\epsilon_n = \frac{2\pi V}{h^3} (2m)^{3/2} \sqrt{\epsilon_n} e^{-\epsilon_n/T} d\epsilon_n, \quad (2.29)$$

which leads to Equation (2.27) after transformation into the lab system. However Cole also shows that if the particles were inside a container and would evaporate through a “small hole”, the resulting energy spectrum of evaporated neutrons should be identical to Weisskopf’s formula (Equation (2.26)).

Terrell had initiated the idea that was able to resolve the problem of the evaporation theory. He has shown that “when allowance is made for the expected distribution of nuclear temperatures of fission fragments, [Weisskopf’s nuclear evaporation theory] predicts an essentially Maxwellian [energy] distribution of fission neutron energies  $[\epsilon_n]$ ” both, in the laboratory system and in the CMS [36, p.527 & 536]. This is found in good agreement with the available empirical data. His basic idea was to include not only a single excitation energy, but a distribution of initial fission fragment excitations. From estimations of the fragment kinetic energies or the number of distributed neutrons,  $E^*$  can be inferred to have an approximately Gaussian shape [37]. The excitation energies  $E^*$  can then, in a simple way, be related to the nuclear temperatures by Weisskopf’s assumption of a degenerated Fermi gas, so that

$$E^* = aT^2 \quad (2.30)$$

where  $a$  is the level spacing constant<sup>14</sup>.

Terrell further noted that the effective residual nucleus energy  $T_Y$  in Equation (2.26) should take into account the energy loss due to the neutron emission (thus yielding  $T_Y(E_\varphi^* - E_B - \epsilon_n)$  instead of  $T_Y(E_\varphi^* - E_B)$ ). In the derivation of a closed expression Kapoor et al. [38, p.291] stated, that the additional effect rises “due to the various states of excitation in which the fragments are left after the emission of the first, second third, etc. neutrons”. Accordingly, with a distribution of the nuclear temperatures  $P(T)$  the emission spectrum (initially from Equation (2.26)) can be written as

$$N(\epsilon_n) = \frac{\int_0^\infty W_n(\epsilon_n) P(T) dT}{\int_0^\infty P(T) dT} = \frac{2\epsilon_n}{T_m^2} \int_0^{T_m} \frac{\exp[-\epsilon_n/T]}{T} dT \approx \frac{2\sqrt{\epsilon_n} \exp[-\epsilon_n/(\frac{8}{9}T_m)]}{\sqrt{\pi}(\frac{8}{9}T_m)^{3/2}}, \quad (2.31)$$

where  $T_m$  is the temperature corresponding to the maximum excitation of a fission fragment. The first equal sign is justified by Terrell’s analysis, who finds a temperature distribution (after shifting due to neutron emission) similar to  $P(T) = 2T/T_m^2$  [36]. The exponential function does

<sup>14</sup>In [32] Weisskopf uses the inverse of  $a$ , thus the relation  $E^* = T^2/a$ .

not have a solution in terms of elementary functions, but through an approximation of the moments of  $N(\epsilon_n)$  one finally finds the centre of mass Maxwellian spectrum<sup>15</sup>. [39–41] Thus, in fact it is shown that Weisskopf's evaporation theory leads to a spectrum that is (approximately) equal to a Maxwellian energy spectrum in the CMS and therefore transforms to a Watt spectrum in the laboratory system.

A final remark should be made regarding the energy dependence of the nucleus formation cross section  $\sigma_{nY}$ . In the derivations above the cross section was assumed to be constant, This seems to be a good approximation for energies in range of several MeV (Weisskopf gives about  $\epsilon_n > 0.8\text{MeV}$  [32, p.302]), but more detailed approaches like the Madland-Nix model [41] give better results, as they take this dependence into account. Furthermore the conservation of angular momentum is not considered in either of these theories. Only a full quantum mechanical treatment like in the Hauser-Feshbach model [42] can account for changes in the density of states that effect the emission probability.

---

<sup>15</sup>In fact Equation (2.31) is a further simplification, as their initial finding of the relation  $\epsilon_n^{5/11} \exp[\dots]$  is approximated by  $\sqrt{\epsilon_n} \exp[\dots]$

## 2.5. Multiplicity Distribution

In addition to the energy spectrum, the distribution of fission neutron numbers can give information on the fission process and properties of the nuclei involved. In the following, two approaches will be presented to calculate multiplicity distributions. Though the results are in good agreement with each other, it is insightful to follow at least the structure of both methods. Critical points in each approach are the distribution of the fragment's excitation energy  $E^*$  and the competition between different de-excitation modes.

Possibly the first derivations of neutron multiplicities were conducted by Leachman in 1956 [43]. Based on Weisskopf's neutron evaporation theory and using various empirical data the emission probabilities and respective energies were determined.

The sum of the excitation of both fission fragments can be deduced through the energy balance of the fission process (which already appeared in a simplified way in Equation (2.3))<sup>16</sup>

$$m(A, Z) + \epsilon_n + E_B = m(A_L, Z_L) + m(A_H, Z_H) + E_K + E^*, \quad (2.32)$$

where the subscripts  $L$  and  $H$  refer to the light and heavy fragment,  $E_K$  to their total kinetic and  $E^*$  to the total excitation energy. Leachman deduced the total excitation energy (distribution) by reversing Equation (2.32) with following input: a) Mass tables for the ground state masses and the binding energy for the fissioning isotope [44, 45] (and extensions of the mass surface to the fragment nuclides), and b) ionization chamber measurements for the kinetic energy distribution of the fragments [46, 47]. The excitation energy distributions of the individual fragments  $P(E_L^*), P(E_H^*)$  are gained by deconvolution of the total excitation, where the assumption was made that the distributions are identical functions and independent other than  $E_L^* + E_H^* = E^*$ . Following the evaporation theory with eq. (2.26), the excitations are used to calculate the neutron emission probability. For simplicity, when emitting several neutrons the nuclear temperature is considered constant in each step. The intermediate result is the multiplicity for a fix pair of fission fragments and the final multiplicities are obtained by a weighted average over the distribution of fragment pairs; to simplify the analysis only three pairs were considered. As can be seen in Figure 2.10 they are, in general, in good agreement with measurements by Diven et al. [48], Hicks et al. [49], Hammel and Kephart [50].

The calculations by Leachman are very complex and involve a large set of experimental parameters, so that Terrell tried find a simpler means of predicting the neutron multiplicities  $P(\nu)$ . With only few assumptions regarding the fission fragment excitation energy Terrell shows that the  $P(\nu)$  is approximately given by a Gaussian distribution. [37]

As in the case of the evaporation theory, in the following it will be assumed that neutrons are emitted whenever energetically possible. Next two assumptions are made that will simplify the calculations significantly: (i) The emission of a neutron reduces a fission fragment's excitation energy by  $\Delta E$ , which is close to the average  $E_0 \equiv \langle \Delta E \rangle$  and (ii) the fission fragment excitations  $P(E_L^*), P(E_H^*)$  are Gaussian distributed with the standard deviation  $E_0 \times \mathcal{O}$  from the mean  $\bar{E}^*$ . The latter assumption seems reasonable on the basis of empirical data (as it was already seen by Leachman) [43, 46, 51]. However, to the best of the author's knowledge, there is no empirical

<sup>16</sup>In Leachman's paper one will find the pair-term  $\delta$  explicitly carried along as a parameter for all formulas. For ease of reading it is dropped in the derivations presented here.

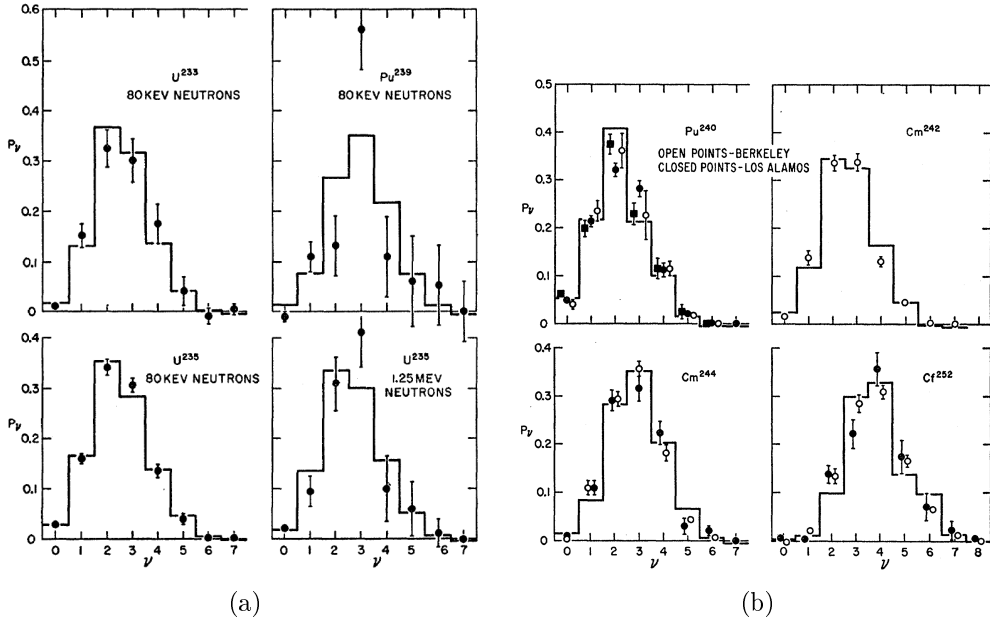


Figure 2.10.: Neutron multiplicities for induced (a) and spontaneous fission (b); calculated results by Leachman are given as bars. Experimental data are shown as filled circles (Diven et al. [48]), open circles (Hicks et al. [49]) and squares (Hammel and Kephart [50]). [43]

evidence or physical reason for  $\Delta E$ , which is the sum of the binding energy  $E_B$  and the neutron's kinetic energy  $\epsilon_n$ , to be approximately constant for all emitted neutrons as stated in (i).<sup>17</sup>

Terrell shows that with only two assumptions (i) and (ii) the the neutron number distribution  $P(\nu)$  can be calculated and that it is relatively insensitive to the distribution of the excitation energy between the fission fragments. In the mathematically simplest case, which is the basis of the calculations below, one fragment carries the total excitation energy  $E^*$ . The cumulative distribution  $D(\nu)$  of  $P(\nu)$  is therefore given by

$$D(\nu) = \sum_{n=0}^{\nu} P(n) = \frac{1}{\mathcal{O}E_0\sqrt{2\pi}} \int_{-\infty}^{(\nu+1)E_0} \exp\left[-\frac{(E^* - \bar{E}^*)^2}{2(\mathcal{O}E_0)^2}\right] dE^*. \quad (2.33)$$

$D(\nu)$  can be expressed only by the average multiplicity  $\bar{\nu}$  and the standard deviation  $\mathcal{O}$  by two substitutions, the first of which is  $t = (E^* - \bar{E}^*)/(\mathcal{O}E_0)$ . Second, with an residual energy of  $E_0/2$  at which no neutron can be emitted anymore, the mean excitation energy is given by  $\bar{E}^* = (\bar{\nu} + 1/2 - b)E_0$ , where  $b$  is a small parameter for the normalization<sup>18</sup>. Equation (2.33) can then be expressed by

$$D(\nu) = \sum_{n=0}^{\nu} P(n) = \frac{1}{\sqrt{2\pi}} \int_{-\infty}^{(\nu - \bar{\nu} + \frac{1}{2} - b)/\mathcal{O}} \exp[-t^2/2] dt = \frac{1}{2} + \frac{1}{2} \operatorname{erf}[(\nu - \bar{\nu} + 1/2 - b)/\mathcal{O}], \quad (2.34)$$

<sup>17</sup>In order to agree with the evaporation spectrum one consequently needs to expect that the first neutrons contribute with higher kinetic energy as they have lower binding energies.

<sup>18</sup>It is necessary to obey the condition  $\sum_0^{\infty} \nu P(\nu) = 1$ , from which the correction parameter  $b$  can be determined to  $b \approx 1/2 - 1/2 \operatorname{erf}[(\bar{\nu} + 1/2)\mathcal{O}]$ . However, for the data observed by Terrell he gives  $b < 10^{-2}$ , thus  $b$  it is almost negligibly small.

where  $\text{erf}(x)$  is the error function. Thus the neutron multiplicities  $P(\nu)$  can be calculated through

$$P(\nu) = D(\nu) - D(\nu - 1), \quad \text{with} \quad \sum_0^{\infty} \nu P(\nu) = 1. \quad (2.35)$$

The calculation of  $P(\nu)$  from the excitation distribution is visualized in Figure 2.11 where the shaded areas refer to  $D(\nu = 0, 1, 2)$  and by eq. (2.35) each interval represents the probability to have an excitation sufficient to emit  $\nu = 0, 1, 2, \dots$  neutrons. The multiplicities  $P(\nu)$  are closely approximated by a Gaussian function which becomes exact in the limit  $E_0/\bar{E}^* \rightarrow 0$ , thus Terrell's illustrative notation will be followed to call it a ‘‘Gaussian’’ distribution; only in this limit the parameter  $\mathcal{O}$  is the stochastic standard deviation, thus we will denote it by the ‘‘width’’ of  $P(\nu)$

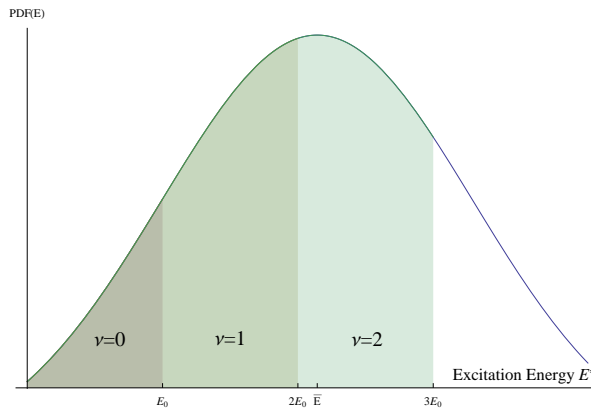


Figure 2.11.: Calculation of the multiplicity distribution  $P(\nu)$  from the excitation energy distribution  $P(\bar{E}^*)$  (eq. (2.33)). The shaded areas refer to  $D(\nu = 0, 1, 2)$  and by eq. (2.35) each interval represents the probability to have an excitation sufficient to emit  $\nu = 0, 1, 2, \dots$  neutrons. Below  $E_0$  no neutron can be emitted.

The resulting ‘‘Gaussian’’ distribution is very simple description of the multiplicities  $P(\nu)$ , but it is established on the simplification that the total excitation energy is with one fragment only, which is very improbable. More reasonable is to assume, just as Leachman does, that the excitation distributions are identical and independent. This will lead to the substitution  $\bar{\nu} \rightarrow \bar{\nu}/2$  and  $\mathcal{O} \rightarrow \mathcal{O}/\sqrt{2}$  in Equation (2.33) and (2.34). The resulting multiplicity distribution  $P(\nu)$  is then a convolution of the individual fragment’s distributions  $P_L(\nu)$  and  $P_H(\nu)$

$$P(\nu) = \sum_{n=0}^{\nu} P_L(n)P_H(\nu - n). \quad (2.36)$$

In conclusion the neutron emission probability  $P(\nu)$  is ‘‘Gaussian’’ distributed and given by Equation (2.35) and (2.36), which involves only two independent parameters  $\bar{\nu}$ , the average neutron multiplicity, and  $\mathcal{O}$ , which is the standard deviation of the excitation energy in unites of  $E_0$ . They were determined by Terrell from empirical data of (A) Diven et al. [48], (B) Hicks et al. [49], (C) Hammel and Kephart [50] and a small amount of unpublished data (D) [52], where the average multiplicity  $\bar{\nu}$  is measured very accurately and  $\mathcal{O}$  was calculated such that

the ‘‘Gaussian’’ function best fits the measured multiplicity distribution. It is interesting to note that Terrell assumed there to be a nearly constant ‘‘width’’  $\mathcal{O}$  for all nuclides; he calculated it to  $\mathcal{O} \approx 1.079(07)$  from a weighted average of twelve measurements with different isotopes. Only for  $^{252}\text{Cf}$  he gives  $\mathcal{O} = 1.207(12)$ . This result is in good agreement with Leachmans calculations, for which Terrell shows that implicitly  $\mathcal{O} \approx 1.08$  was used and similar results were gained by Cohen’s [53] with  $\mathcal{O} \approx 1.13$ . The calculations by Terrell can be seen in Table 2.3 and Figure 2.12.

Terrell’s results for a fixed neutron multiplicity ‘‘width’’  $\mathcal{O}$  are clearly an approximation only as they do not take into account variations of  $\mathcal{O}$  with the incident neutron energy  $\epsilon_n$ . Experimental data compilations by Zucker and Holden [54] however clearly show that  $\mathcal{O}$  varies with  $\epsilon_n$ , where usually the multiplicity distribution broadens with the higher energies  $d\mathcal{O}/d\epsilon_n > 0$ . Though smaller in magnitude, additional corrections are expected as Leachman and Terrell only implement de-excitation by neutrons. Only a model like Haus-Feshbach-Theory including the competition between neutrons and gammas will be able to account for the resulting deviations. [55]

Table 2.3.: ‘‘Width’’ of fission neutron multiplicity distributions  $P(\nu)$ . For fission induced neutrons the incident energy is given, references to the data are found in the text. The quantities  $\mathcal{O}$  and the variance  $Var(\nu)$  are measures for the width<sup>19</sup> of  $P(\nu)$ . The last two lines give a weighted average of  $\mathcal{O}$ . [37]

Fissioning nuclide	Reference	$\bar{\nu}$	Experimental data	
			$\mathcal{O}$	$Var(\nu) = \langle \nu^2 \rangle_{Av} - \bar{\nu}^2$
$\text{Pu}^{242}$	B	$2.18 \pm 0.09$	$1.069 \pm 0.035$	$1.19 \pm 0.07$
$\text{Pu}^{240}$	A - C	$2.26 \pm 0.05$	$1.109 \pm 0.012$	$1.28 \pm 0.03$
$\text{Pu}^{236}$	B	$2.30 \pm 0.19$	$1.11 \pm 0.11$	$1.28 \pm 0.21$
$\text{Pu}^{238}$	B	$2.33 \pm 0.08$	$1.115 \pm 0.023$	$1.30 \pm 0.05$
$\text{U}^{235} + n$ (80 keV)	A	$2.47 \pm 0.03$	$1.072 \pm 0.021$	$1.22 \pm 0.04$
$\text{U}^{233} + n$ (80 keV)	A	$2.58 \pm 0.06$	$1.041 \pm 0.041$	$1.16 \pm 0.08$
$\text{Cm}^{242}$	B	$2.65 \pm 0.09$	$1.053 \pm 0.013$	$1.18 \pm 0.03$
$\text{U}^{235} + n$ (1.25 MeV)	C	$2.65 \pm 0.07$	$1.04 \pm 0.06$	$1.15 \pm 0.12$
$\text{U}^{238} + n$ (1.5 MeV)	C	$2.65 \pm 0.09$	$1.23 \pm 0.08$	$1.56 \pm 0.18$
$\text{Cm}^{244}$	A, B	$2.82 \pm 0.05$	$1.036 \pm 0.018$	$1.15 \pm 0.05$
$\text{Pu}^{239} + n$ (80 keV)	A	$3.05 \pm 0.08$	$1.14 \pm 0.07$	$1.38 \pm 0.14$
$\text{U}^{235} + n$ (4.8 MeV)	C	$3.20 \pm 0.08$	$1.20 \pm 0.06$	$1.51 \pm 0.13$
$\text{Cf}^{252}$	A, B	$3.86 \pm 0.07$	$1.207 \pm 0.012$	$1.54 \pm 0.04$
All			$1.110 \pm 0.006$	
All but $\text{Cf}^{252}$			$1.079 \pm 0.007$	

<sup>19</sup>According to Terrell  $\mathcal{O}$  can be uniquely determined by the variance  $Var(\nu)$ . Terrell’s derivation of  $\mathcal{O}$  is not given and the authors attempts to reproduce the calculations with the usual formula for a Gaussian distribution  $\mathcal{O} = \sqrt{Var(\nu)}$  lead to deviations of about 4%. Similar deviations were gained by fitting a ‘‘Gaussian’’ according to Equation (2.35) or (2.36) to the data. Maybe the data sets had different weighting according to their measurement uncertainty.

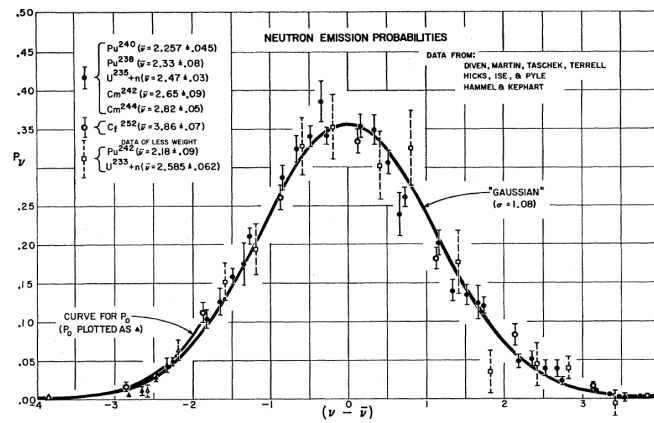


Figure 2.12.: Neutron multiplicities. The continuous line is for a “Gaussian” distribution with  $\sigma \approx 1.08$ . Reference to the experimental data is given in the text; standard deviations are shown. [37]

# 3

## Chapter 3.

# Implementation in MCNPX-PoliMi

## 3.1. Neutron Multiplicities

MCNPX-PoliMi samples the neutron (and also gamma) multiplicities from appropriate distributions for each spontaneous and neutron-induced fission event. The following section expresses the understanding based on the user's manual [56] and the most comprehensive paper published on this issue [6]. Where information was not available we assume that MCNPX-PoliMi follows earlier codes like MCNPX and MCNP-DSP.

For the implemented neutron multiplicities, two general groups can be distinguished:

- The spontaneous fission neutron multiplicity data is, according to Pozzi et al. [6, p.120], adopted for evaluations conducted by Santi and Miller [57]. Their method and the data for  $^{238}\text{U}$  and  $^{240}\text{Pu}$  refer back to an early work of Holden and Zucker [58]. The (re-)evaluation was necessary to account for improved measurements of the average multiplicity  $\bar{\nu}$  since the initial experiments were conducted. As the average  $\bar{\nu}$  can be measured more precisely independent of the individual probabilities  $P(\nu)$ , both are still connected by  $\bar{\nu} = \sum \nu P(\nu)$ , a change on  $\bar{\nu}$  requires a subsequent update of  $P(\nu)$ . More information on the method and the resulting distributions for  $^{238}\text{U}$  and  $^{240}\text{Pu}$  can be found in Appendix A.
- For neutron-induced fission, no direct reference on the source data was available. The manual lists three options for the multiplicity data,

	Description in manual [56, p.14]		Assumed source
(1)	“Terrell; nubar $[\bar{\nu}]$ from MCNPX libraries”	$\Leftrightarrow$	Terrell [37] (with $\bar{\nu}$ from MCNPX libraries)
(2)	“Zucker & Holden for $^{235}\text{U}$ , $^{238}\text{U}$ and $^{239}\text{Pu}$ ”	$\Leftrightarrow$	Zucker and Holden [54] <sup>1</sup>
(3)	“Gwin & al. $^{235}\text{U}$ , Zucker & Holden $^{238}\text{U}$ and $^{239}\text{Pu}$ .”	$\Leftrightarrow$	Gwin et al. [59] and [54].

In (1) the multiplicity distribution  $P(\nu)$  is calculated by the “Gaussian” with the energy-independent “width”  $\mathcal{O}$  as introduced by Terrell. The parameters can be found in Table 2.3. One finds that only for  $^{235}\text{U} + n$  it is ambiguous which data was taken, as there are three sets for different neutron incident energies  $E_n$ ; for no reference was given we assume that

<sup>1</sup>Zucker and Holden [54] includes one set of energy dependent data and a second for  $E_n \approx 0$ . As other information was not available, we assume the implementation follows Tim Valentine's (ORNL) polynomial fit in MCNP-DSP [60, p.5] the energy dependent values are taken. - Note Added in Proof: This was confirmed by Enrico Padovani (Polytechnic of Milan), pers. comm., 26.08.2013.

MCNPX-PoliMi follows MCNPX, which implements the “width”  $\mathcal{O} = 1.072$  corresponding to 80 keV neutrons [61, p.5-67]. The second parameter, the average neutron multiplicity  $\bar{\nu}$ , is gained as a function of  $E_n$ . This function is sampled directly from the Evaluated Nuclear Data File (ENDF)<sup>2</sup> and is shown in Figure 3.1.

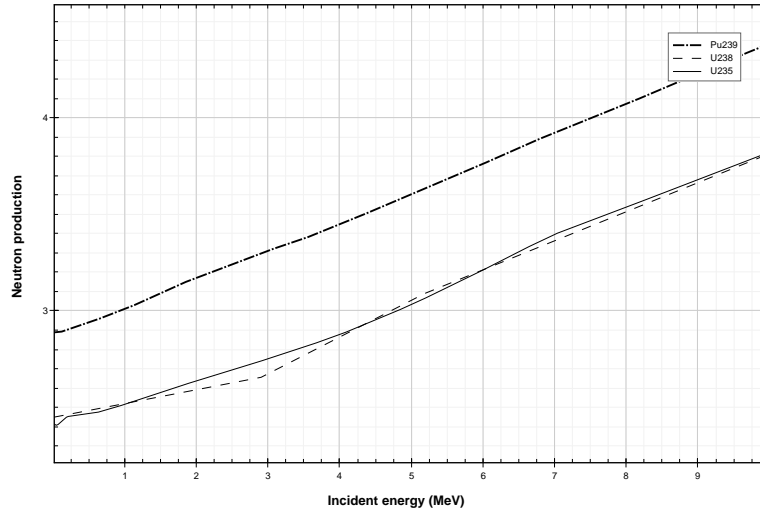


Figure 3.1.: Average neutron multiplicity  $\bar{\nu}$  of  $^{235}\text{U}$  (solid line)  $^{238}\text{U}$  (dashed) and  $^{239}\text{Pu}$  (dashed and dotted) as a function of the incident neutron energy  $E_n$ . Retrieved from [29, 30, 62, MT456]

For (2) we assume<sup>3</sup> that Zucker and Holden’s energy dependent data is implemented. It should be remarked that their analysis includes the induced fission of  $^{235}\text{U}$ ,  $^{238}\text{U}$  and  $^{239}\text{Pu}$  only. Following a suggestion by Frehaut [63] and subsequently its inclusion in MCNP-DSP [60], it is possible that the fitted values of  $P(\nu)$  for the three isotopes above are used also for the other uranium and plutonium isotopes. Otherwise Terrell’s data is taken. Is it not known to the author which method is used in MCNPX-PoliMi. However, for many application only the first three mentioned nuclides are of significance.

Gwin et al. [59] made very precise multiplicities measurements of  $^{233}\text{U}$ ,  $^{235}\text{U}$ , Pu  $^{239}\text{U}$  and  $^{241}\text{U}$  with thermal neutrons. Consistently with the implementation in MCNP-DSP [60, p.5] we assume that the measurements for  $^{235}\text{U}$  are additionally called up with setting (3); for the multiplicities of  $^{235}\text{U}$  with neutrons of higher energy and the whole set of  $^{238}\text{U}$  and  $^{239}\text{Pu}$  the data of Zucker and Holden are adopted by MCNPX-PoliMi.

## 3.2. Energy Dependence of Neutron-Induced Fission Multiplicities for Fast Neutrons

While there is a fair amount of published literature on spontaneous and induced fission multiplicities with neutrons between thermal energies and some tens of keV, probably the first (and possibly the only) published data on fast neutrons is based on experiments by Frehaut and his

<sup>2</sup>Andreas Enqvist (University of Michigan), pers. comm., 13.08.2013.

<sup>3</sup>Note Added in Proof: This was confirmed by Enrico Padovani (Polytechnic of Milan), pers. comm., 26.08.2013. See footnote 1.

co-workers<sup>4</sup>. The experiment covers the induced fission multiplicities of  $^{235}\text{U}$ ,  $^{238}\text{U}$  and  $^{239}\text{Pu}$  between incident energies in the range of 1-25 MeV, however, due to poor counting statistic they were only published later by Zucker and Holden [54] who smoothed the data. They found reliable data for  $P(\nu)$  between 0-10 MeV with an extrapolation of measurements<sup>5</sup> by Frehaut et al. for  $^{238}\text{U}$  and an additional data (by [58] and other evaluations, see [54, p.14]) for the thermal energy ranges of  $^{238}\text{U}$  and  $^{239}\text{Pu}$ . [54]

Figure 3.2 shows the energy dependent multiplicities  $P(\nu)$  for  $^{239}\text{Pu}$  gained by Zucker and Holden [54], which are assumed to be implemented in Option (2) of MCNPX-PoliMi's source specification card and the calculations with the "Gaussian" of "width"  $\mathcal{O}$  by Terrell [37] and  $\bar{\nu}(E)$  from ENDF. For higher incident energies  $E_n$  the average neutron multiplicity  $\bar{\nu}$  increases, as more energy is available for de-excitation of the nucleus by multiple neutron emissions. Moreover, because Terrell's parameter for the "width" of the distribution  $\mathcal{O}$  is constant, unlike Zucker and Holden's distribution which broadens with higher energies, there is a difference between the two sets of  $P(\nu)$  that increases with the incident energy  $E_n$ . The energy dependent multiplicity distributions  $P(\nu)$   $^{235}\text{U}$  and  $^{238}\text{U}$  qualitatively show similar characteristics and are given in Appendix B Figure B.2 and B.3.

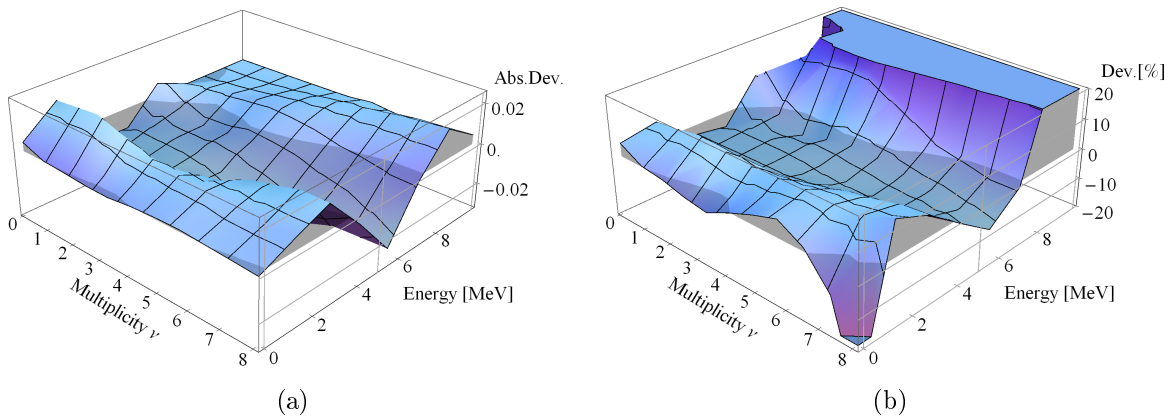


Figure 3.2.: Dependence of the neutron-induced fission multiplicities  $P(\nu)$  on the incident energy  $E_n$  for  $^{239}\text{Pu}$ . The graphs show the absolute (a) and relative (b) difference between the analysis by Zucker and Holden [54] and calculations for the parameters of Terrell [37]. In this representation the data points (given only at integer values by [54]) are connected by a smooth function and the shaded area is the difference to zero. Relative deviations of more than  $\pm 20\%$  are reached only at very low values of  $P(\nu)$  and therefore not shown here.

A quantitative description of the differences between the two sets for the neutron multiplicity distribution  $P(\nu)$  can be compared for a model system. We have chosen a configuration where we analyse the deviation between [54] and Terrell [37] on a microscopic scale under following simplifications for the calculation: (i) The sample consists of one isotope only, (ii) there are only spontaneous and induced fission reactions, (for instance  $(\alpha, n)$ -reactions and scattering are not

<sup>4</sup>J. Frehaut and coworkers at the Commissariat a l'Energie Atomique, Dentre d'etudes de Bruyeres le Chatel" as cited in [54]. See also [64].

<sup>5</sup>As fission cross-section of  $^{238}\text{U}$  is very small below the effective fission threshold of about 1 MeV, there is comparatively little data available.

considered), (iii) all neutrons are emitted with an energy given by the fission spectrum  $W_n(E_n)$  (Eq.(2.31)).

Moreover, the definition of a meaningful quantity for the comparison is required. Many of the multiplicity measurement techniques are based on the work of Böhnel [65] to determine the nuclear material mass in a sample through the first three factorial moments [66]; thus, they will be chosen for the comparison.

The first three factorial moments are defined by

$$\langle \nu \rangle = \sum_{\nu=0}^{\max} \nu P(\nu), \quad (3.1)$$

$$\langle \nu(\nu - 1) \rangle = \sum_{\nu=0}^{\max} \nu(\nu - 1)P(\nu), \quad (3.2)$$

$$\langle \nu(\nu - 1)(\nu - 2) \rangle = \sum_{\nu=0}^{\max} \nu(\nu - 1)(\nu - 2)P(\nu). \quad (3.3)$$

If one assumes Zucker and Holden's analysis to give the most accurate energy dependence of  $P(\nu)$ , the aim is to calculate the deviation  $\Delta_{P(\nu)}$  of the multiplicity distribution by using the parameters proposed by Terrell. Without loss of generality, the derivations are explicitly applied to the first factorial moment<sup>6</sup>  $\langle \nu \rangle$ . With the simplifications (i) to (iii), the deviation  $\Delta_{\langle \nu \rangle}$  of  $\langle \nu \rangle$  is given by a weighted average over: first, the fission spectrum  $W_n(E_n)$  (Eq.(2.31)), corresponding to the fraction of neutrons in the sample with the energy  $E_n$  and second, probability for these neutrons to induce fission, given by the fission cross section  $\sigma_{nf}(E_n)$

$$\Delta_{\langle \nu \rangle} = \sum_{E_n=0}^{\max=10\text{MeV}} (\langle \nu \rangle_{E_n}^{\text{Zucker\&Holden}} - \langle \nu \rangle_{E_n}^{\text{Terrell}}) W_n(E_n) w_{\sigma_{nf}}(E_n), \quad (3.4)$$

where  $\langle \nu \rangle_{E_n}$  is the first factorial moment for a fixed energy  $E_n$  and  $w_{\sigma_{nf}}(E_n)$  is the fission cross section, normalized to unity. As the multiplicities are published in the Zucker and Holden data [54, Table III-V] for integer energies only, both weighting factors are discretised by integration over the intervals  $[E_n \pm 1/2 \text{ MeV}]$  for  $E_n \geq 1 \text{ MeV}$  and  $[0, 0.5] \text{ MeV}$  for  $E_n = 0 \text{ MeV}$ . All additional input parameters are retrieved for the relevant nuclide from the ENDF/B-VII.1 evaluations [29, 30, 62]. They are given by the energy spectrum  $W_n(E_n)$ , the cross section  $\sigma_{nf}(E_n)$ , and for the calculation of the moments of Terrell's distribution by Eq.(2.35), the conversion tables from incident energies  $E_n$  to  $\bar{\nu} = \langle \nu \rangle$ . The resonance region of the fission cross section, which is visible below 30keV for the data sets used, is approximated by an  $1/\sqrt{E_n}$  dependency. Finally, the weighted relative deviation  $\Delta_{\langle \nu \rangle, rel}$  is calculated by

$$\Delta_{\langle \nu \rangle, rel} = \frac{\Delta_{\langle \nu \rangle}}{\sum_{E_n=0}^{\max} \langle \nu \rangle_{E_n}^{\text{Zucker\&Holden}} W_n(E_n) w_{\sigma_{nf}}(E_n)}. \quad (3.5)$$

Table 3.1 lists the weighted relative deviations  $\Delta_{\langle \nu \rangle, rel}$  on the factorial moments for neutron-induced fission multiplicities of  $^{235}\text{U}$ ,  $^{238}\text{U}$  and  $^{239}\text{Pu}$  between (1) Terrell and (2) Zucker and

<sup>6</sup>For higher moments simply replace  $\langle \nu \rangle$  with the desired quantity. Besides, it should be noted that the factorial moments defined in Equation (3.1-3.3) are taken for a fixed energy

Holden. For  $^{235}\text{U}$  the deviations of the two additional parameters  $\mathcal{O}$  given by Terrell [37] are calculated, however we assume MCNPX-PoliMi follows MCNPX to implement  $\mathcal{O}=1.072$ . The high variability of the deviations, about  $\pm 10\%$  on the third moment for calculations with the different values of  $\mathcal{O}$  further illustrate the error that may be introduced with an energy independent multiplicity “width”.

Table 3.1.: Weighted relative deviations  $\Delta_{\langle\nu\rangle,rel}$  between Terrell [37] and Zucker and Holden [54] for the first three moments of the multiplicity distribution  $P(\nu)$  implemented in MCNPX-PoliMi. For  $^{235}\text{U}$  the deviations of the two additional data sets given by Terrell are calculated, however we assume MCNPX-PoliMi follows MCNPX to implement  $\mathcal{O}=1.072$

	$\Delta_{\langle\nu\rangle,rel} [\%]$				
	$^{235}\text{U}$			$^{238}\text{U}$	$^{239}\text{Pu}$
	$\mathcal{O}=1.04$	1.072	1.20		
$\langle\nu\rangle$	0.11	0.08	-0.12	0.10	0.03
$\langle\nu(\nu-1)\rangle$	2.90	1.73	-3.29	-1.86	0.49
$\langle\nu(\nu-1)(\nu-2)\rangle$	10.96	7.58	-7.04	-2.42	3.04

The third option implemented in MCNPX-PoliMi, which adds the precise measurements by Gwin et al. [59] to the  $^{235}\text{U}$  multiplicities for thermal neutrons to the data by Zucker and Holden [54], may give an additional improvement. The deviations are calculated as before, only that Gwin is the reference value in Eq. 3.5. It can be seen from the comparison in Table 3.2 that Zucker and Holden underestimate the first moments of the thermal neutron multiplicity by about 1%.

Table 3.2.: Weighted relative deviations  $\Delta_{\langle\nu\rangle,rel}$  between Zucker and Holden [54] and Gwin [59] for the first three moments of the multiplicity distribution  $P(\nu)$  of  $^{235}\text{U}$  implemented in MCNPX-PoliMi.

	$\Delta_{\langle\nu\rangle,rel} [\%]$
	$^{235}\text{U}$
$\langle\nu\rangle$	-0.96
$\langle\nu(\nu-1)\rangle$	-1.44
$\langle\nu(\nu-1)(\nu-2)\rangle$	-1.07

The energy dependence of the “width”  $\mathcal{O}$  found by Zucker and Holden is plotted in Figure 3.3, where  $\mathcal{O}$  was calculated as the root of the variances of  $P(\nu)$  listed in [54, Table III-V]. Although desirable, due to the lack of a pattern between shapes for the different nuclides it seems difficult generalise the energy dependence of  $\mathcal{O}$ ; Appendix B includes the values for this plot in Table B.1. This is also reflected in a remark by Zucker and Holden on the analysis of the experimental variation of the multiplicities  $P(\nu)$  [54, p.12]

The more we have delved into the details of  $P(\nu)$  the more it seems to be so that such systematics as are noticed (e.g. Terrell [37], et al.) are true only in a fairly

approximate sense and are not necessarily accurate enough relations to be useful in many technical applications, such as neutron correlation counting.

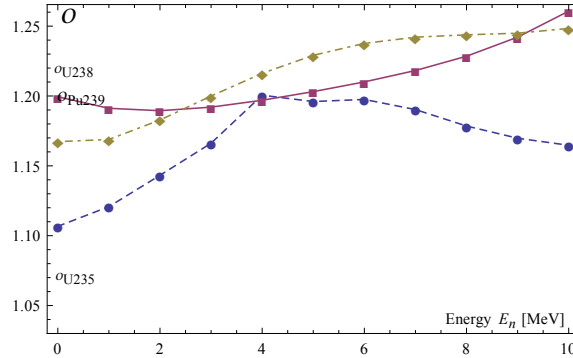


Figure 3.3.: Experimental energy dependence of the multiplicity distribution “width”  $\mathcal{O}$  for  $^{235}\text{U}$  (stars),  $^{238}\text{U}$  (triangles) and  $^{239}\text{U}$  (diamonds) calculated from the variances quoted in the analysis of Zucker and Holden [54, Table III-V]. The calculated values of Terrell [37] are given as a comparison to the right of the y-axes.

## Discussion

The analysis up to this point suggests that if the multiplicity distribution  $P(\nu)$  is described by a “Gaussian”, the corresponding “width”  $\mathcal{O}$  should depend on the incident neutron energy  $E_n$ . At first this seems to be in apparent conflict with the work by Lestone [67], who finds, for almost identical source data, that below approximately 10 MeV the “width”  $\mathcal{O}$  can be assumed to be independent of  $E_n$ . The author became aware of the analysis by Lestone [67] only just before the submission of this study, however a preliminary comparison of both approaches can be drawn.

In his study Lestone [67] compares calculations based on a “Gaussian” function to experimental data by Soleilhac et al. [64]. This data is also the source of the analysis by Zucker and Holden [54]; we are, just as Lestone [67, p.1], not aware of any other measurements for the multiplicities  $^{235}\text{U}$ ,  $^{238}\text{U}$  and  $^{239}\text{Pu}$  for fast neutrons. Lestone takes a different approach to fit  $\mathcal{O}$  to empirical data by which it is attempted to minimize  $\chi^2$  directly of the factorial moments instead of minimizing it for the measured distribution of  $P(\nu)$ ; Figure 3.4 represents such a fit for  $^{239}\text{U}$ .

The calculations of Lestone [67] are seemingly in good agreement with the experimental data [64], but contrary to Lestone who concludes that the “width”  $\mathcal{O}$  is independent of  $E_n$ , we calculate a deviation for the third moment of about 3% (see Table 3.1). To explain the inconsistency, in Table 3.3 we calculate the difference between the “Gaussians” used. This yields typically to less than 1%. However, a first estimate by manually reading the data of Figure 3.4 indicates<sup>7</sup>, that the deviation between Lestone’s fit and the experimental data is also in the order of 3% to 5%. Consequently, this preliminary result indicates that the sparse empirical evidence is, at least, inconclusive concerning the energy dependence of the “width”  $\mathcal{O}$ .

<sup>7</sup>The estimate is based on the the two data points circled in Figure 3.4 that show a deviation of about  $0.7/15 \approx 4.7$  for the first and  $1/30 \approx 1.3$  for the second point, respectively.

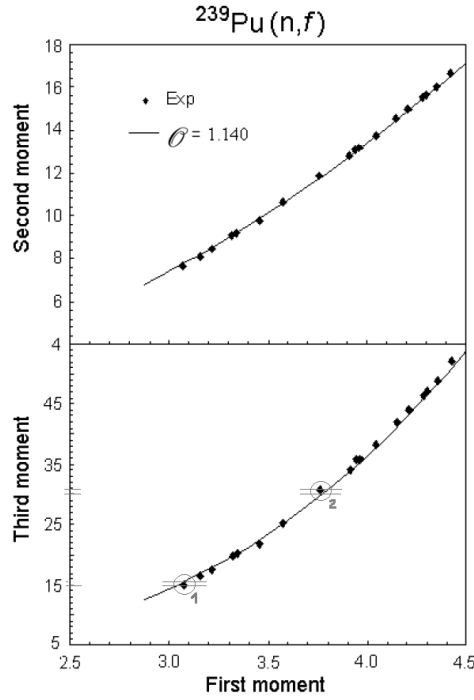


Figure 3.4.: The second and third factorial moments as a function of the first factorial moment for  $^{239}\text{Pu}$ . The solid line shows the calculations by Lestone [67] for fix “width”  $\mathcal{O} = 1.140$ , independent of the incident energy. The experimental data taken from [64], where we have selected two points (circled) to roughly estimate the uncertainty. Adapted from [67, Fig.3].

Table 3.3.: Relative difference between the first three factorial moments of  $P(\nu)$  as calculated by this study from parameters given in [37], and the analysis of [67, Table IV]. For  $^{238}\text{U}$  the data is not listed in [67].

$\mathcal{O}$	$^{235}\text{U}$			$^{239}\text{Pu}$		
	Terrell	Lestone	Rel. Diff. [%]	Terrell	Lestone	Rel. Diff. [%]
	1.072	1.088		1.140	1.140	
$\langle \nu \rangle$	2.42738	2.413	0.5923	2.87739	2.875	0.0830
$\langle \nu(\nu - 1) \rangle$	4.6776	4.635	0.9107	6.77401	6.6738	1.47933
$\langle \nu(\nu - 1)(\nu - 2) \rangle$	6.75058	6.778	-0.4062	12.5169	12.528	-0.0886

### 3.3. Neutron Energy Distribution

After the multiplicity distribution is sampled over one of the above mentioned data sets, MCNPX-PoliMi determines the fission neutron energy distribution  $P(\epsilon_n)$  [6]. For induced fission both distributions are implemented independently of each other [6]; following the implementation in MCNPX [61, H-1ff], we assume that the neutron energy is sampled from a Watt spectrum. In case of spontaneous fission data from a model developed by Lemaire et al. [68] is used [6], which is presented in this section. If not noted otherwise the derivations will follow Lemaire et al. [68].

The approach taken by [68] relies on Weisskopf's evaporation theory and is in principle similar to Leachman's calculations [43], which were introduced in section 2.5. However, their Monte Carlo simulation is able to give much more details on the fission process, for example one can extract the neutron energy for a specific multiplicity  $\epsilon_n(\nu)$ . Though the model can in general be applied to all isotopes, provided the necessary input parameters are sufficiently well known, the paper reported results only on neutron-induced fission of  $^{235}\text{U}$  (at  $E_n = 0.53\text{MeV}$ ) and the spontaneous fission of  $^{252}\text{Cf}$ . Accordingly references to the data in the following section refer to these isotopes only.

The total excitation energy of both fission fragments  $E_{\text{tot}}^*$  is obtained from the energy balance, Equation (2.32), where the fragment masses<sup>8</sup> for the light and heavy pair  $A_L, A_H$  are gained from an atomic mass evaluation [69]. More than 70 different pairs of  $A_L$  and  $A_H$  were sampled from an experimental pre-neutron emission fission fragment mass distribution [70, 71]; the corresponding charge and kinetic energy distributions were assumed to be Gaussians with parameters from [72] and [70, 71] respectively.

A crucial point that accounts for different results in several calculations is again the total excitation energy partition between the light and heavy fragments. In the model of [68], two hypotheses are considered:

- (H1) Light and heavy fragment share the same nuclear temperature at scission. It follows from the Fermi gas model Eq. (2.30) for a level density parameter<sup>9</sup>  $a$  proportional to the mass number  $A$  (for a derivation see e.g. [73, p.59]), that the initial excitation energy of a given fission fragment is

$$E^* = aT^2, a \propto A \rightarrow E_{\text{tot}}^* = E_L^* + E_H^* = a_L T^2 + a_H T^2 = a_L E_L^* + \frac{a_H}{a_L} E_L^*$$

$$E_{L,H}^* = E_{\text{tot}}^* \frac{1}{1 + \frac{a_{H,L}}{a_{L,H}}} \quad (3.6)$$

- (H2) Experimental data of the de-excitation is used to infer the initial excitation of each fragment, namely, the average neutron multiplicities  $\bar{\nu}_{\text{exp}}(A)$ , neutron and gamma energies  $\langle \epsilon_n \rangle_{\text{exp}}(A)$  and  $\bar{E}_{\text{exp},\gamma}(A)$

$$E_{L,H} = E_{\text{tot}}^* \frac{\bar{\nu}_{\text{exp}}(A_{L,H}) \langle \eta \rangle_{L,H} + \bar{E}_{\text{exp},\gamma}(A_{L,H})}{\sum_{i=L,H} [\bar{\nu}_{\text{exp}}(A_i) \langle \eta \rangle_i + \bar{E}_{\text{exp},\gamma}(A_i)]}, \quad (3.7)$$

<sup>8</sup>Though not explicitly mentioned, it will be assumed that Lemaire et al. [68] also gained the neutron binding energy from [69].

<sup>9</sup>For an explicit definition of  $a$ , see Lemaire et al. [68, p.5].

where  $\langle \eta \rangle_{L,H}$  is the average energy removed from the fragment per emitted neutron. It is the sum of neutron CMS-energy  $\langle \epsilon_n \rangle_{exp}(A)$  and the binding energy, which was averaged over the pairing effect for the removal of two neutrons, so that

$$\langle \eta \rangle_{L,H} = \langle \epsilon_n \rangle_{exp}(A_{L,H}) + \frac{1}{2} E_{B_{2n}}(A_{L,H}, Z_{L,H}). \quad (3.8)$$

Additionally Lemaire et al. [68] assumed that the ratio of energies removed by neutrons and gammas for both fragments is equal, which is, at least, not unreasonable regarding the de-excitation models. The input parameters are taken from [74–76].

Given the nuclear temperature  $T_{H,L}$  by the Fermi model  $E^* = aT^2$  and the excitation energy by (H1) or (H2), the emission probability for a neutron with a given kinetic energy is obtained by sampling over the Weisskopf spectrum, Eq. (2.26). Neutrons are emitted until the the excitation energy of the residual nucleus is less than neutron separation and pairing energy. Here also Terrell's correction explained in section 2.4.2 is implemented, which states that the residual nucleus excitation should take into account the emitted neutron energy thus yielding  $E^*(A-1, Z) = E^*(A, Z) - E_B - \epsilon_n$ ; this is important for the simulation between the competition between neutron and  $\gamma$  emission at lower energies.

Besides, it should be mentioned that Lemaire et al. [68] assume a constant inverse cross section  $\sigma_{nY}(\epsilon_n)$ . The spectrum in the laboratory system is by sampling for each nucleus over all emission angles under the usual assumption of isotropic emission in CMS. An advantage over previously discussed models however is, that not only an average, but the exact recoil energy of the residual nucleus can be taken into account.

Figure 3.5 gives the neutron energy spectrum calculated with each hypothesis for  $^{252}\text{Cf}$  (a) in the CMS and (b) laboratory system respectively. As a comparison also the Madland-Nix (=Los Alamos) model [41] calculations are shown. There is a close correspondence between the spectrum gained with equal temperatures at scission (H1) and the CMS calculations of the Madland-Nix model. The same degree of agreement is reached in the laboratory system with the experimental data by [77] for both hypothesis. As Lemaire et al. [68] noted, the second hypothesis (H2), which produces a too hard spectrum, could be improved for the high energy tail if an energy dependent cross section as in the Madland-Nix model was taken into account.

The neutron-induced energy spectrum of  $n(0, 53 \text{ MeV}) + ^{235}\text{U}$  is not represented very well by the approach of Lemaire et al. [68]. This can be seen in Figure 3.6, that shows the neutron energy spectrum with both hypotheses in (a) the CMS and (b) the laboratory system respectively. Whilst in the CMS (H1) is still in reasonable agreement with the Madland-Nix model [Madland1982] in the laboratory system none of the assumptions can reproduce the experimental data by [78] (though the Madland-Nix Model does). We have to conjecture that a lack of sufficiently precise input data is the reason for the derivations for energies of neutron-induced fission, thus leading to an independent sampling of the multiplicities in MCNPX-PoliMi. As Pozzi et al. [6] state, “the available data were not deemed sufficient to develop a generalized model (including [...] neutron-induced fission) of the dependence of the energy spectrum on the number of neutron emitted in the fission event.”

The final neutron energy spectra implemented in MCNPX-PoliMi for two spontaneous fissioning nuclides,  $^{252}\text{Cf}$  and  $^{240}\text{Pu}$ , are presented in Figure 3.7, where the spectra are shown for each of the possible multiplicities of a fission. To generate them,  $10^8$  spontaneous-fission events were sampled according to the method described above (and additional input parameters for  $^{240}\text{Pu}$ ).

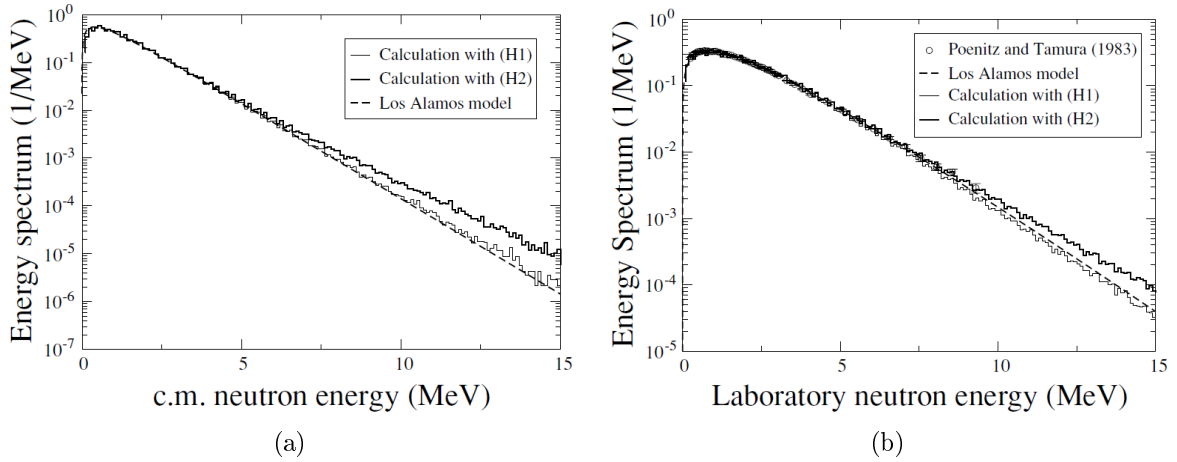


Figure 3.5.: Neutron energy spectrum for the spontaneous fission of  $^{252}\text{Cf}$  in (a) the fission fragment CMS and (b) the laboratory system. The thin line are results of Lemaire et al. obtained when assuming equal temperature at scission (H1) and the thick line when partitioning of the excitation energy is based on experimental data for the de-excitation (H2). For a comparison to the two hypothesis, the results of the Madland-Nix model (=Los Alamos model) are shown as a dashed line. Both hypothesis are in good agreement with the experimental data by [77] in the laboratory system. Reproduced from [68, p.5].

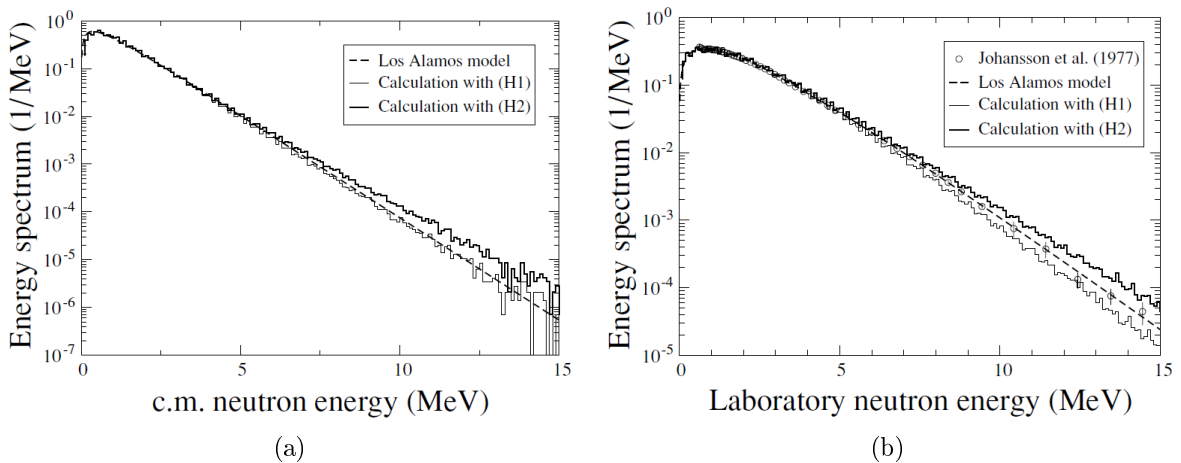


Figure 3.6.: Neutron energy spectrum for the neutron-induced fission  $n(0, 53 \text{ MeV}) + ^{235}\text{U}$  in (a) the fission fragment CMS and (b) the laboratory system. Experimental data for the laboratory system are from [78]. Reproduced from [68, p.4].

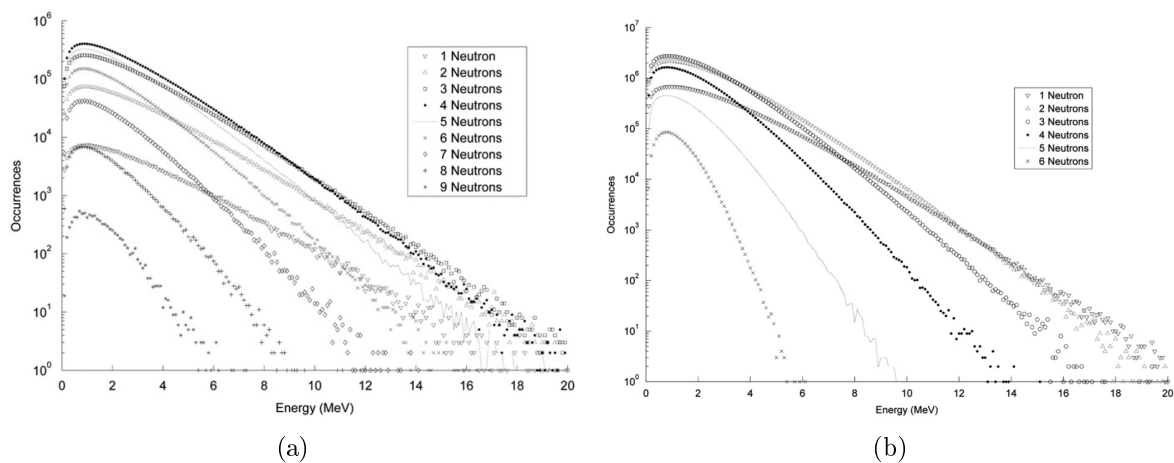


Figure 3.7.: Neutron energy spectrum as a function of various multiplicities for the spontaneous fission implemented in MCNPX-PoliMi for (a)  $^{252}\text{Cf}$  and (b)  $^{240}\text{Pu}$ ; the distributions were generated by simulating  $10^8$  fission events for each isotope. Reproduced from [6, p.121].



# 4

## Chapter 4.

---

# Conclusions

Given the isotopic composition from gamma measurements, the detection of neutron multiplicities can be used to determine the mass of nuclear material. It requires accurate knowledge of the neutron multiplicity distribution of a fission process. This study has summarized the understanding of the physical background of neutron multiplicities, determined influence factors like the incident particle energy and reviewed the implementation in MCNPX-PoliMi.

The fission neutrons spectra resulting from Weisskopf's evaporation theory [32] was shown to follow a Maxwellian energy distribution in the centre of mass system, if allowance is made for the expected distribution of fission fragment excitations. The Maxwellian transform into a Watt spectrum in the laboratory framework [33]. A further refinement of this theory is given by the Madland-Nix model [41], which lifts the previously used simplification of a constant "inverse" cross section.

The work of Terrell [37] was revisited, which approximates the multiplicity distribution by a "Gaussian" function (see Section 2.5 for the definition). There are two parameters, the average neutron multiplicity  $\bar{\nu}$  and the "width"  $\mathcal{O}$  of the multiplicity distribution. For induced fission Terrell predicts that only  $\bar{\nu}$  depends on the incident neutron energy.

MCNPX-PoliMi samples the neutron multiplicities from appropriate distributions for each spontaneous and neutron-induced fission event. Where information on the implementation was not available it was assumed that MCNPX-PoliMi follows earlier codes like MCNPX and MCNP-DSP. The spontaneous fission neutron multiplicity data is adopted for evaluations conducted by Santi and Miller [57]. For the distribution of induced fissions either the calculations by Terrell [37] can be used, or empirical data of Soleilhac et al. [64] which was analysed by Zucker and Holden [54]. To the best of the author's knowledge the latter is the only published set of multiplicity measurements for fast neutrons.

For spontaneously fissioning nuclides and thermal to low energy neutrons the calculations of the multiplicity distribution are in good agreement with empirical data. However, a comparison with the data analysed by Zucker and Holden [54] for incident energies between 0 and 10 MeV yields significant differences.

A quantitative description of the deviations between the multiplicity distributions predicted by Terrell, and by Zucker and Holden has been developed in a model system. For simplicity, the sample consists of a single isotope, and only spontaneous and neutron induced fission reactions

are considered. The resulting deviations are below  $\pm 0.2\%$  for the first moment, below  $\pm 1.9\%$  for the second moment, but for the third moment yield up to approximately  $7.6\%$  for  $^{235}\text{U}$ ,  $-2.4\%$  for  $^{238}\text{U}$  and  $3\%$  for  $^{239}\text{Pu}$ .

Consequently, this study indicates that if the multiplicity distribution  $P(\nu)$  is described by a “Gaussian”, the corresponding “width”  $\mathcal{O}$  of  $P(\nu)$  should depend on the incident neutron energy  $E_n$ . This might be in conflict with the work by Lestone [67], who finds that below approximately 10 MeV the “width”  $\mathcal{O}$  can be assumed to be independent of  $E_n$ . However, a preliminary calculation of this study shows that the deviations between Lestone’s calculations and the experimental data are also in the order of  $3\%$  to  $5\%$  for the third moments.

Considering the sparse empirical evidence, it is thus inconclusive whether the “width”  $\mathcal{O}$  depends on the incident neutron energy. In the absence of further measurements of the multiplicity distribution  $P(\nu)$  of fast neutrons, a comparison of actual simulations conducted with the different distributions implemented in MCNPX-PoliMi may give further insight on this issue. Finally, the reliability of the results could be checked against multiplicity counting measurements of nuclear material samples.

# Acknowledgements

First and foremost I would like to thank my supervisor Gerald Kirchner and my advisor Malte Göttsche and, for his warm-hearted support, Frederik Postelt. From the beginning of my involvement with the Centre for Science and Peace Research I have received great support and was allowed to work on many interesting tasks that finally made me decide to write my bachelor thesis here. I can hardly express the gratitude for introducing me to a whole new world – with all the friends and colleagues living in it. There is a multitude (or multiplicity?) of activities I've had the pleasure to enjoy with you, whether it was talking about different modes of de-excitation of fission fragments, simply spending a nice evening with Moritz in a pub in Oslo or leading students to dismantle the bomb.

I would also like to thank Götz Neuneck for co-supervising my thesis and the manifold contributions to the project that I'm now working in.

The librarians at the Physik-Bibliothek Jungiusstraße were of extraordinary help in digging for many books and journals that had been covered by the dust of time.

This thesis would not have been possible in this form without the revelation of Arne Schmäser, bringing good tea to my life, every moment we able to; Florian Sprung for his most constructive feedback on my thesis draft until late at night and Johannes Kühn for sharing insight to the art of pronouncing Zsebkendő, Sophie Terhorst and Simone Rassman for being who they are, and all my colleagues and friends for Your support and suggestions.

Finally, but first in my heart, my parents are due my deep gratitude for their continued interest and encouragement throughout my studies. The broad education that I was able to enjoy while growing up has proven invaluable.

Thank You!



# Bibliography

- [1] N. Ensslin. *Passive Nondestructive Assay of Nuclear Materials*, chapter Principles of Neutron Coincidence Counting, pages 457–492. In Pan [18], March 1991. URL [http://www.osti.gov/energycitations/product.biblio.jsp?osti\\_id=5428834](http://www.osti.gov/energycitations/product.biblio.jsp?osti_id=5428834).
- [2] S. N. Kile and H. M. Kristensen. *SIPRI Yearbook 2013: Armaments, Disarmament and International Security (SIPRI Yearbook Series)*, chapter 6. World Nuclear Forces - Overview, page 284. Oxford University Press, USA, 2013. ISBN 019967843X.
- [3] T. R. Rutherford and J. H. McNeilly. Measurements on Material to be Stored at the Mayak Fissile Material Storage Facility. In *Proceedings of the 41st Annual Meeting of the Institute for Nuclear Materials Management*, 2000.
- [4] N. Ensslin, W. C. Harker, M. S. Krick, D. G. Langner, M. M. Pickrell, and J. E. Stewart. Application Guide to Neutron Multiplicity Counting. Technical Report LA-13422-M, Los Alamos National Laboratory, November 1998. URL [http://www.osti.gov/bridge/product.biblio.jsp?osti\\_id=1679](http://www.osti.gov/bridge/product.biblio.jsp?osti_id=1679).
- [5] X-5 Monte Carlo Team. MCNP – A General N-Particle Transport Code, Version 5. Technical Report LA-UR-03-1987, Los Alamos National Laboratory, April 24 (Revised 2/1/2008) 2003.
- [6] S. A. Pozzi, S.D. Clarke, W.J. Walsh, E.C. Miller, J.L. Dolan, M. Flaska, B.M. Wieger, A. Enqvist, E. Padovani, J.K. Mattingly, D.L. Chichester, and P. Peerani. MCNPX-PoliMi for Nuclear Nonproliferation Applications. *Nuclear Instruments and Methods in Physics Research Section A: Accelerators, Spectrometers, Detectors and Associated Equipment*, 694(0):119 – 125, 2012. doi: <http://dx.doi.org/10.1016/j.nima.2012.07.040>.
- [7] E. Rutherford, F. W. Aston, J. Chadwick, C. D. Ellis, G. Gamow, R. H. Fowler, O. W. Richardson, and D. R. Hartree. Discussion on the Structure of Atomic Nuclei. *Proceedings of the Royal Society A: Mathematical, Physical and Engineering Sciences*, 123(792):373–390, Apr 1929. doi: [10.1098/rspa.1929.0074](https://doi.org/10.1098/rspa.1929.0074).
- [8] C. F. von Weizsäcker. Zur Theorie der Kernmassen (On the theory of nuclear masses). *Zeitschrift für Physik (Journal of Physics)*, 96:431–458, 1935.
- [9] H. A. Bethe and R. F. Bacher. Nuclear Physics A. Stationary States of Nuclei. *Rev. Mod. Phys.*, 8:82–229, Apr 1936. doi: <http://link.aps.org/doi/10.1103/RevModPhys.8.82>.
- [10] N. Bohr and J. A. Wheeler. The Mechanism of Nuclear Fission. *Physical Review*, 56:426–450, Sep 1939. doi: [10.1103/PhysRev.56.426](https://doi.org/10.1103/PhysRev.56.426). URL <http://link.aps.org/doi/10.1103/PhysRev.56.426>.
- [11] N. D. Cook. *Models of the Atomic Nucleus, Unification Through a Lattice of Nucleons*, volume 2nd ed. Springer Berlin Heidelberg, 2010. doi: [10.1007/978-3-642-14737-1](https://doi.org/10.1007/978-3-642-14737-1).

- [12] K. Bethge, G. Walter, and B. Wiedemann. *Kernphysik, Eine Einführung*. Springer-Lehrbuch. Springer, Berlin [u.a.], 3., aktualisierte und erw. Aufl. edition, 2008. doi: <http://dx.doi.org/10.1007/978-3-540-74567-9>.
- [13] B. Povh, K. Rith, C. Scholz, and F. Zetsche. *Teilchen und Kerne. Eine Einführung in die physikalischen Konzepte*. Springer-Lehrbuch. Springer Berlin Heidelberg, 2009. doi: [10.1007/978-3-540-68080-2](https://doi.org/10.1007/978-3-540-68080-2). URL <http://dx.doi.org/10.1007/978-3-540-68080-2>.
- [14] L. Meitner and O. R. Frisch. Disintegration of Uranium by Neutrons: a New Type of Nuclear Reaction. *Nature*, 143(3615):239–40, February 11 1939. doi: [10.1038/143239a0](https://doi.org/10.1038/143239a0).
- [15] N. Bohr and F. Kalckar. On the Transmutation of Atomic Nuclei by Impact of Material Particles, I. General Theoretical Remarks. *Kgl. Danske Vid. Selskab. Math. Fys. Medd.*, 14(10):1–40, 1937. URL <http://www.sdu.dk/en/Bibliotek/matfys>.
- [16] H. J. Krappe and K. Pomorski. *Theory of Nuclear Fission*. Number 838 in Lecture notes in physics. Springer, Heidelberg [u.a.], 2012. ISBN 9783642235146. doi: [10.1007/978-3-642-23515-3](https://doi.org/10.1007/978-3-642-23515-3).
- [17] D. C. Hoffman and M. M. Hoffman. Post-Fission Phenomena. *Annual Review of Nuclear Science*, 24(1):151–208, 1974. doi: [10.1146/annurev.ns.24.120174.001055](https://doi.org/10.1146/annurev.ns.24.120174.001055). URL <http://www.annualreviews.org/doi/abs/10.1146/annurev.ns.24.120174.001055>.
- [18] Passive Nondestructive Assay of Nuclear Materials. Technical Report PANDA, LA-UR-90-732, Nuclear Regulatory Commission, Washington, DC (United States). Office of Nuclear Regulatory Research; Los Alamos National Lab., NM (United States), March 1991. URL [http://www.osti.gov/energycitations/product.biblio.jsp?osti\\_id=5428834](http://www.osti.gov/energycitations/product.biblio.jsp?osti_id=5428834).
- [19] S. Frankel and N. Metropolis. Calculations in the Liquid-Drop Model of Fission. *Physical Review*, 72:914–925, Nov 1947. doi: [10.1103/PhysRev.72.914](https://doi.org/10.1103/PhysRev.72.914). URL <http://link.aps.org/doi/10.1103/PhysRev.72.914>.
- [20] R. Vandenbosch and G. T. Seaborg. Considerations on the Probability of Nuclear Fission. *Physical Review*, 110:507–513, Apr 1958. doi: [10.1103/PhysRev.110.507](https://doi.org/10.1103/PhysRev.110.507). URL <http://link.aps.org/doi/10.1103/PhysRev.110.507>.
- [21] N. E. Holden and Darleane C. H. Spontaneous Fission Half-Lives for Ground-State Nuclide (Technical Report). *Pure and Applied Chemistry*, 72(8):1525–1562, 2000. doi: [10.1351/pac200072081525](https://doi.org/10.1351/pac200072081525). URL <http://dx.doi.org/10.1351/pac200072081525>.
- [22] G. Audi, O. Bersillon, J. Blachot, and A.H. Wapstra. The Nubase evaluation of nuclear and decay properties. *Nuclear Physics A*, 729(1):3–128, Dec 2003. doi: [10.1016/j.nuclphysa.2003.11.001](https://doi.org/10.1016/j.nuclphysa.2003.11.001). URL <http://dx.doi.org/10.1016/j.nuclphysa.2003.11.001>.
- [23] E. K. Hyde, I. P., and G. T. Seaborg. *The Nuclear Properties of the Heavy Elements, III, Fission Phenomena*. Prentice-Hall International Series in chemistry. Prentice-Hall, Englewood Cliffs NJ, 1964.
- [24] N. Bohr. Neutron Capture and Nuclear Constitution. *Nature*, 137:344–348, February 29 1936. doi: [10.1038/137344a0](https://doi.org/10.1038/137344a0).

- [25] John M. Blatt and Victor F. Weisskopf. *Theoretical Nuclear Physics*. Wiley [u.a.], New York, 1952.
- [26] A. J. Cole. *Statistical Models for Nuclear Decay, From Evaporation to Vaporization*. Taylor & Francis, 2000. doi: 978-0750305129.
- [27] Samuel Glasstone and Milton C. Edlund. *The Elements of Nuclear Reactor Theory*. Van Nostrand, Toronto [u.a.], 3rd printing edition, 1955.
- [28] P. G. Young, M. B. Chadwick, A. C. Kahler, T. Kawano, H. Derrien, and L. C. Leal D. Wiarda. ENDF/B-VII.1 Evaluation, Material 9440 (Pu-240), 2010.
- [29] P. G. Young, M. B. Chadwick, R. E. MacFarlane, W. B. Wilson, D. G. Madland, P. Talou, T. Kawano, H. Derrien, G. de Saussure, T. Nakawa, D. A. Brown, and J. Pruet. ENDF/B-VII.1 Evaluation, Material 9437 (Pu-239), 2010.
- [30] P. G. Young, M. B. Chadwick, R. E. MacFarlane, W. B. Wilson, D. G. Madland, P. Talou, T. Kawano, L. C. Leal, H. Derrien, N. M. Larson, R. Q. Wright, D. A. Brown, and J. Pruet. ENDF/B-VII.1 Evaluation, Material 9228 (U-235), 2010.
- [31] L. Frenkel. On the Solid Model of Heavy Nuclei. *Physikalische Zeitschrift der Sowjetunion*, 9:533–536, 1936.
- [32] V. Weisskopf. Statistics and Nuclear Reactions. *Physical Review*, 52:295–303, Aug 1937. doi: 10.1103/PhysRev.52.295. URL <http://link.aps.org/doi/10.1103/PhysRev.52.295>.
- [33] B. E. Watt. Energy Spectrum of Neutrons from Thermal Fission of U-235. *Physical Review*, 87:1037–1041, Sep 1952. doi: 10.1103/PhysRev.87.1037. URL <http://link.aps.org/doi/10.1103/PhysRev.87.1037>.
- [34] D. L. Hill. The Neutron Energy Spectrum from U-235 Thermal Fission. *Physical Review*, 87:1034–1037, Sep 1952. doi: 10.1103/PhysRev.87.1034. URL <http://link.aps.org/doi/10.1103/PhysRev.87.1034>.
- [35] N. Feather. Emission of Neutrons from Moving Fission Fragments, (unpublished report) BM-148, British Mission. As cited in [33]. 1942.
- [36] J. Terrell. Fission Neutron Spectra and Nuclear Temperatures. *Physical Review*, 113:527–541, Jan 1959. doi: 10.1103/PhysRev.113.527. URL <http://link.aps.org/doi/10.1103/PhysRev.113.527>.
- [37] J. Terrell. Distributions of Fission Neutron Numbers. *Physical Review*, 108:783–789, Nov 1957. doi: 10.1103/PhysRev.108.783. URL <http://link.aps.org/doi/10.1103/PhysRev.108.783>.
- [38] S. S. Kapoor, R. Ramanna, and P. N. Rama Rao. Emission of Prompt Neutrons in the Thermal Neutron Fission of U-235. *Physical Review*, 131:283–296, Jul 1963. doi: 10.1103/PhysRev.131.283. URL <http://link.aps.org/doi/10.1103/PhysRev.131.283>.
- [39] Le Couteur. In *Proc. Phys. Soc.*, volume A65, page 718, 1952.
- [40] K. J. Le Couteur and J. M. B. Lang. In *Proc. Phys. Soc.*, volume A67, page 586, 1954.

- [41] D. G. Madland and J. R. Nix. New Calculation of Prompt Fission Neutron Spectra and Average Prompt Neutron Multiplicities. *Nuclear Science and Engineering*, 81(2):213–271, 6 1982.
- [42] W. Hauser and H. Feshbach. The Inelastic Scattering of Neutrons. *Physical Review*, 87:366–373, Jul 1952. doi: 10.1103/PhysRev.87.366. URL <http://link.aps.org/doi/10.1103/PhysRev.87.366>.
- [43] R. B. Leachman. Emission of Prompt Neutrons from Fission. *Physical Review*, 101:1005–1011, Feb 1956. doi: 10.1103/PhysRev.101.1005. URL <http://link.aps.org/doi/10.1103/PhysRev.101.1005>.
- [44] R. A. Glass. Radiation Laboratory Report UCRL-2560 (unpublished). As cited in [43]. 1954.
- [45] J.R. Huizenga and L.B. Magnusson. *Masses, neutron and proton binding energies of the heavy elements*, volume Argonne National Laboratory Report 5158. U.S. Atomic Energy Commission, 1953.
- [46] D. C. Brunton and G. C. Hanna. Energy Distribution of Fission Fragments from U-235 and U-233. *Canadian Journal of Research*, 28a(2):190–227, 1950. doi: 10.1139/cjr50a-019. URL <http://www.nrcresearchpress.com/doi/abs/10.1139/cjr50a-019>.
- [47] D. C. Brunton and W. B. Thompson. Energy Distribution of Fission Fragments from Pu-239. *Canadian Journal of Research*, 28a(5):498–508, 1950. doi: 10.1139/cjr50a-040. URL <http://www.nrcresearchpress.com/doi/abs/10.1139/cjr50a-040>.
- [48] B. C. Diven, H. C. Martin, R. F. Taschek, and J. Terrell. Multiplicities of Fission Neutrons. *Physical Review*, 101:1012–1015, Feb 1956. doi: 10.1103/PhysRev.101.1012. URL <http://link.aps.org/doi/10.1103/PhysRev.101.1012>.
- [49] D. A. Hicks, J. Isle, R. V. Pyle, and B. Choppin, G. and Harvey. Correlations between the Neutron Multiplicities and Spontaneous Fission Modes of Californium-252. *Physical Review*, 105:1507–1511, Mar 1957. doi: 10.1103/PhysRev.105.1507. URL <http://link.aps.org/doi/10.1103/PhysRev.105.1507>.
- [50] J. E. Hammel and J. F. Kephart. Distribution of the Number of Prompt Neutrons from the Spontaneous Fission of Pu-240. *Physical Review*, 100:190–192, Oct 1955. doi: 10.1103/PhysRev.100.190. URL <http://link.aps.org/doi/10.1103/PhysRev.100.190>.
- [51] J. S. Fraser and J. C. D. Milton. Distribution of Prompt-Neutron Emission Probability for the Fission Fragments of U-233. *Physical Review*, 93:818–824, Feb 1954. doi: 10.1103/PhysRev.93.818. URL <http://link.aps.org/doi/10.1103/PhysRev.93.818>.
- [52] B. C. Diven, H. C. Martin, R. F. Taschek, and J. Terrell. (unpublished) As cited in [37].
- [53] B. L. Cohen, A. F. Cohen, and C. D. Coley. Energy Distribution of Mass-97 Fission Fragments from Thermal-Neutron Fission of Uranium-235. *Physical Review*, 104(4):1046–1053, Nov 1956. doi: 10.1103/PhysRev.104.1046. URL <http://link.aps.org/doi/10.1103/PhysRev.104.1046>.
- [54] M.S. Zucker and N.E. Holden. Energy Dependence of the Neutron Multiplicity  $P(v)$  in Fast Neutron Induced Fission of U-235, U-238, and Pu-239. In *Conference: American Nuclear*

- Society annual meeting, Reno, NV, USA, 15 Jun 1986*, volume Report Number: BNL-38491; CONF-860610-34, OSTI ID: 6974950, page 36. Brookhaven National Lab., Upton, NY (USA);, 1986. URL [http://www.osti.gov/bridge/product.biblio.jsp?query\\_id=0&page=0&osti\\_id=6974950&Row=19&formname=basicsearch.jsp](http://www.osti.gov/bridge/product.biblio.jsp?query_id=0&page=0&osti_id=6974950&Row=19&formname=basicsearch.jsp).
- [55] D.G. Madland. Post-scission fission theory: Neutron emission in fission. In *Proceedings of the Workshop on Nuclear Reaction Data and Nuclear Reactors - Physics, Design and Safety*, number LA-UR-97-2657, page 11, NM (United States), 11 1997. Los Alamos National Lab.; USDOE Office of Energy Research, Washington, DC (United States). doi: 10.2172/548904.
- [56] E. Padovani, S. A. Pozzi, S. D. Clarke, and E. C. Miller. Introduction To MCNP-PoliMi. Technical report, Politecnico di Milano, Milan, Italy and University of Michigan, Ann Arbor, USA.
- [57] P. Santi and M. Miller. Reevaluation of Prompt Neutron Emission Multiplicity Distributions for Spontaneous Fission. *Nuclear science and engineering*, 168(2):190–199, 2008.
- [58] N. E. Holden and M. S. Zucker. A Re-Evaluation of the Average Prompt Neutron Emission Multiplicity (Nubar) Values from Fission of Uranium and Transuranium Nuclides. *IAEA Advisory Group Mtg. Neutron Standard Reference Data*, (IAEA-TECDOC-335, BNL 35513): 248–255, November 1984.
- [59] R. Gwin, R. R. Spencer, , and R. W. Ingle. Measurements of the Energy Dependence of Prompt Neutron Emission from U-233, U-235, Pu-239, and Pu-241 for  $E_n = 0.005$  to 10 eV Relative to Emission from Spontaneous Fission of Cf-252. *Nuclear Science and Engineering*, 87:381–404, 1984.
- [60] T.E. Valentine. MCNP-DSP Users Manual. Technical Report ORNL/TM-13334/R2, Oak Ridge National Lab., Jan 19 2001.
- [61] MCNPX User's Manual. Version 2.7.0. Technical Report LA-CP-11-00438, Los Alamos National Laboratory, April 2011.
- [62] P. G. Young, M. B. Chadwick, R. E. MacFarlane, W. B. Wilson, D. G. Madland, P. Talou, T. Kawano, H. Derrien, A. Courcelle L. C. Leal, and N. M. Larson. ENDF/B-VII.1 Evaluation, Material 9237 (U-238), 2010.
- [63] J. Frehaut. Neutron Multiplicity Distribution in Fast Neutron-Induced Fission. In *Proceedings of a Consultants' Meeting on Physics of Neutron Emission in Fission, Mito, Japan*, number INDC(NDS)-220, page 81, 1988.
- [64] M. Soleilhac, J. Frehaut, and J. Gauriau. Energy dependence of  $\nu_p$  for neutron-induced fission of  $^{235}\text{U}$ ,  $^{238}\text{U}$  and  $^{239}\text{Pu}$  from 1.3 to 15 MeV. *Journal of Nuclear Energy*, 23(5):257 – 282, 1969. ISSN 0022-3107. doi: [http://dx.doi.org/10.1016/0022-3107\(69\)90060-4](http://dx.doi.org/10.1016/0022-3107(69)90060-4). URL <http://www.sciencedirect.com/science/article/pii/0022310769900604>.
- [65] K. Böhnel. The Effect of Multiplication on the Quantitative Determination of Spontaneously Fissioning Isotopes by Neutron Correlation Analysis. *Nuclear Science and Engineering*, 90: 75–82, 1985.
- [66] P. Santi, D.H. Beddingfield, and D.R. Mayo. Revised prompt neutron emission multiplicity distributions for  $^{236}\text{Pu}$ ,  $^{238}\text{Pu}$ . *Nuclear Physics A*, 756(3–4):325 – 332, 2005. ISSN

- 0375-9474. doi: <http://dx.doi.org/10.1016/j.nuclphysa.2005.04.002>. URL <http://www.sciencedirect.com/science/article/pii/S0375947405005610>.
- [67] J. P. Lestone. Energy and Isotope Dependence of Neutron Multiplicity Distributions. (LA-UR-05-0288), 2005. URL <http://library.lanl.gov/cgi-bin/getfile?LA-UR-05-0288.pdf>.
- [68] S. Lemaire, P. Talou, T. Kawano, M. B. Chadwick, and D. G. Madland. Monte Carlo approach to sequential neutron emission from fission fragments. *Phys. Rev. C*, 72:024601, Aug 2005. doi: 10.1103/PhysRevC.72.024601. URL <http://link.aps.org/doi/10.1103/PhysRevC.72.024601>.
- [69] A. H. Wapstra, G. Audi, and C. Thibault. The Ame2003 atomic mass evaluation: (I). Evaluation of input data, adjustment procedures and (II). Tables, graphs and references. *Nuclear Physics A*, 729(1):(I)129–336; (II)337–676, 2003. ISSN 0375-9474. doi: <http://dx.doi.org/10.1016/j.nuclphysa.2003.11.002>, [10.1016/j.nuclphysa.2003.11.003](http://dx.doi.org/10.1016/j.nuclphysa.2003.11.003).
- [70] F.-J. Hambsch and S. Oberstedt. Investigation of the far asymmetric region in  $^{252}\text{Cf}(\text{sf})$ . *Nuclear Physics A*, 617(3):347 – 355, 1997. ISSN 0375-9474. doi: [http://dx.doi.org/10.1016/S0375-9474\(97\)00040-7](http://dx.doi.org/10.1016/S0375-9474(97)00040-7).
- [71] H. W. Schmitt, J. H. Neiler, and F. J. Walter. Fragment Energy Correlation Measurements for  $^{252}\text{Cf}$  Spontaneous Fission and  $^{235}\text{U}$  Thermal-Neutron Fission. *Physical Review*, 141: 1146–1160, Jan 1966. doi: 10.1103/PhysRev.141.1146. URL <http://link.aps.org/doi/10.1103/PhysRev.141.1146>.
- [72] W. Reisdorf, J.P. Unik, H.C. Griffin, and L.E. Glendenin. Fission Fragment K X-Ray Emission and Nuclear Charge Distribution for Thermal Neutron Fission of U-233, U-235, Pu-239 and Spontaneous Fission of Cf-252. *Nuclear Physics A*, 177(2):337 – 378, 1971. ISSN 0375-9474. doi: [http://dx.doi.org/10.1016/0375-9474\(71\)90297-1](http://dx.doi.org/10.1016/0375-9474(71)90297-1). URL <http://www.sciencedirect.com/science/article/pii/0375947471902971>.
- [73] Joachim Alexander Maruhn, Paul-Gerhard Reinhard, and Eric Suraud. *Simple Models of Many-Fermion Systems*. Springer-Verlag, 2010. ISBN 978-3-642-03838-9. doi: 10.1007/978-3-642-03839-6. URL <http://dx.doi.org/10.1007/978-3-642-03839-6>.
- [74] C. Budtz-Jørgensen and H.-H. Knitter. Simultaneous investigation of fission fragments and neutrons in Cf-252 (SF). *Nuclear Physics A*, 490(2):307 – 328, 1988. ISSN 0375-9474. doi: [http://dx.doi.org/10.1016/0375-9474\(88\)90508-8](http://dx.doi.org/10.1016/0375-9474(88)90508-8). URL <http://www.sciencedirect.com/science/article/pii/0375947488905088>.
- [75] K. Nishio, Y. Nakagome, H. Yamamoto, and I. Kimura. Multiplicity and energy of neutrons from U-252 ( $n_{th,f}$ ) fission fragments. *Nuclear Physics A*, 632(4):540 – 558, 1998. ISSN 0375-9474. doi: [http://dx.doi.org/10.1016/S0375-9474\(98\)00008-6](http://dx.doi.org/10.1016/S0375-9474(98)00008-6). URL <http://www.sciencedirect.com/science/article/pii/S0375947498000086>.
- [76] F. Pleasonton, R. Ferguson, and H. Schmitt. Prompt Gamma Rays Emitted in the Thermal-Neutron-Induced Fission of U-235. *Physical Review C*, 6(3):1023–1039, Sep 1972. doi: 10.1103/PhysRevC.6.1023. URL <http://dx.doi.org/10.1103/PhysRevC.6.1023>.
- [77] W. P. Poenitz and T. Tamura. In *Proceedings of the International Conference on Nuclear Data for Science and Technology, Antwerp, Belgium, 1982*, number the average energy results

- form a Maxwellian fit to the complete experimental spectrum, page 465. [Peidl Publishing, Dordrecht, Holland, 1983], 1983.
- [78] P. I. Johansson and B. Holmqvist. *Nuclear Science and Engineering*, 62:695, 1977.
- [79] A.G. Popeko, V.I. Smirnov, G.M. Ter-Akop'yan, B.V. Fefilov, and L.P. Chelnokov. Multiplicity of prompt neutrons in spontaneous fission of  $^{238}\text{U}$ . *Soviet Journal of Nuclear Physics*, 25:245–247, 1976.
- [80] S. Huang, J. Chen, and H. Huan. Multiplicity of Prompt Neutrons from Spontaneous Fission of Uranium-238. *Acta Phys. Sin.*, 23(1):46–51, 1974.
- [81] E. Baron, J. Frehaut, and M. Soleilhac F. Ouvry. Neutrons Prompts de Fission mesure de  $\langle v \rangle$  et des Probabilites  $P(v)$  d' Emission de  $v$  Neutrons. In *Nuclear Data For Reactors, Proceedings of a Conference on Nuclear Data*, volume 2, pages 57–66, Oktober 17-21. 1966.
- [82] Y. Wang and J. Xu. Probability of Prompt Neutron Emission from Spontaneous Fission of Pu-240. *Acta Phys. Sin.*, 23(1):38–45, 1974. URL <http://wulixb.iphy.ac.cn/CN/Y1974/V23/I1/38>.
- [83] H. Zhang, Z. Liu, S. Ding, and S. Liu. The Average Number of Prompt Neutrons and the Distributions of Prompt Neutron Emission Number for Spontaneous Fission of Plutonium-240 Curium-242 and Curium-244. *Nuclear Science and Engineering*, 86:315–331, 1984.
- [84] J. W. Boldeman and M. G. Hines. Prompt Neutron Emission Probabilites Following Spon and Thermal Neutron Fission. *Nuclear Science and Engineering*, 91:114–116, 1985.



# A

## Appendix A.

# Re-Evaluation of Spontaneous Neutron Multiplicities

The neutron multiplicities  $P(\nu)$  for spontaneous fission in MCNPX-PoliMi are taken from Santi and Miller [57], who re-evaluated the distributions to account for improved measurements of the average multiplicity  $\bar{\nu}$  since the initial experiments were conducted. As the average  $\bar{\nu}$  can be measured more precisely independent of the individual probabilities  $P(\nu)$ , both are still connected by  $\bar{\nu} = \sum \nu P(\nu)$ , a change on  $\bar{\nu}$  requires a subsequent update of  $P(\nu)$ . The method for the re-evaluation was derived in an earlier compilation by Holden and Zucker [58] and is explained in the following. [58]

In order to determine the neutron multiplicities  $P(\nu)$  from experiments, knowledge of the detector efficiency  $\epsilon$  is essential. The later can in turn be determined from the average neutron multiplicity  $\bar{\nu}$  of well known calibration samples<sup>1</sup> by

$$g = \epsilon \bar{\nu} q, \quad (\text{A.1})$$

where  $q$  is the known fission rate and  $g$  the gross count rate for the calibration sample. By equation (A.1)  $\epsilon$  is inversely related to  $\bar{\nu}$  and if the value initially used to calibrate the detector changes, so should the detector efficiency  $\epsilon$  (and therefore the detected neutron number probabilities). To correct the emission probability  $P(\nu)$  of  $\nu$  neutron for this fact, first the probability  $Q_n$  of actually observing  $n$  neutrons in a measurement is reconstructed with the old values  $\epsilon'$  for the detector efficiency

$$Q_n = \sum_{\nu} P(\nu) \left[ \frac{\nu!}{n!(\nu-n)!} \right] \epsilon'^n (1 - \epsilon')^{\nu-n}. \quad (\text{A.2})$$

Then a set of  $P(\nu)$  can be calculated that is both consistent with the updated value of  $\bar{\nu}$  (and  $\epsilon$ ) and the initially distribution of observed neutrons  $Q_n$ . Therefore equation (A.2) is inverted and used with the updated values, thus yielding

$$P(\nu) = \sum_n Q_n \left[ \frac{n!}{\nu!(n-\nu)!} \right] \epsilon^{-n} (\epsilon - 1)^{n-\nu}. \quad (\text{A.3})$$

---

<sup>1</sup>“The most careful experiments on  $[\bar{\nu}]$  have been those which compare the thermal neutron fission value for the fissile nuclide with the  $[\bar{\nu}]$  value for the spontaneous fission of  $^{252}\text{Cf}$  [58, p.248].

After the neutron multiplicities  $P(\nu)$  from various experiments (if available) have been transformed in this way, any remaining difference is attributed to measurement uncertainties. The average values and corresponding standard deviations for  $^{238}\text{U}$  and  $^{240}\text{Pu}$  are derived (if within one sigma from the mean) from two [79, 80] and seven [48–50, 81–84] different measurement respectively; Table A.1 lists the results. Except for [79], who applied  $^3\text{He}$  proportional counters, all experiments used liquid scintillator detectors.

Table A.1.: Neutron multiplicities for spontaneous fission from  $^{238}\text{U}$  and  $^{240}\text{Pu}$ . The prime is used to denote that the mean values are derived after the data sets were adjusted to the updated value of  $\langle\nu\rangle$ . Reference to original experiments is given in the table. Reproduced from [58].

	$^{238}\text{U}$ [79, 80]			$^{240}\text{Pu}$ [48–50, 81–84]		
	Mean	Std.Dev		Mean	Std.Dev	
		abs.	[%]		abs.	[%]
$P_0$	.0481677	.0054	11.21	.0631852	.0033	5.223
$P_1$	.2485215	.0403	16.22	.2319644	.0019	0.8191
$P_2$	.4253044	.0839	19.73	.3333230	.0061	1.830
$P_3$	.2284094	.0263	11.51	.2528207	.0060	2.373
$P_4$	.0423438	.0108	25.51	.0986461	.0031	3.143
$P_5$	.0072533	.0011	15.17	.0180199	.0017	9.434
$P_6$				.0020406	.0018	88.21
$\langle\nu\rangle^*$	1.9900000*	.03	1.5	2.1540000*	.005	0.232
$\langle\nu(\nu - 1)\rangle$	2.8743	.1411	4.909	3.7889	.0290	0.7654
$\langle\nu(\nu - 1)(\nu - 2)\rangle$	2.8219	.4810	17.05	5.2105	.1492	2.863

# B

## Appendix B.

# Supplementary Data on the Energy Dependence of $P(\nu)$

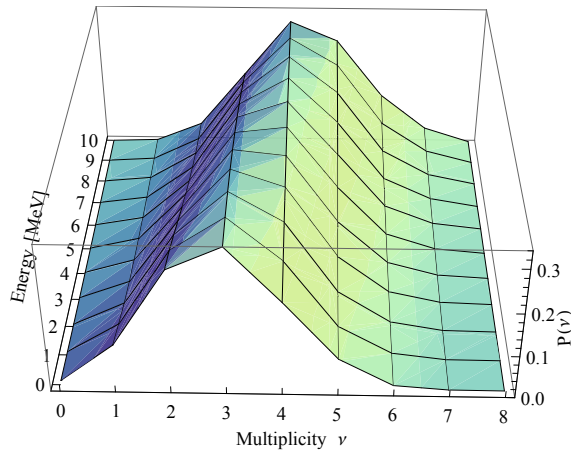


Figure B.1.: Empirical dependence of the neutron-induced fission multiplicities  $P(\nu)$  on the incident energy  $E_n$  for  $^{239}\text{Pu}$ . In this representation the data points (given only at integer values by [54]) are connected by a smooth function.

$E_n$	$\mathcal{O}$										
	$n=0$	1	2	3	4	5	6	7	8	9	10
$^{235}\text{U}$	1.107	1.121	1.143	1.166	1.201	1.196	1.198	1.190	1.179	1.170	1.165
$^{238}\text{U}$	1.199	1.191	1.189	1.192	1.197	1.203	1.210	1.218	1.228	1.242	1.261
$^{239}\text{Pu}$	1.167	1.169	1.183	1.200	1.216	1.229	1.238	1.242	1.244	1.245	1.248

Table B.1.: Empirical energy dependence of the multiplicity distribution “width”  $\mathcal{O}$  for  $^{235}\text{U}$ ,  $^{238}\text{U}$  and  $^{239}\text{U}$  calculated from the variances quoted in the analysis of Zucker and Holden [54, Table III-V].

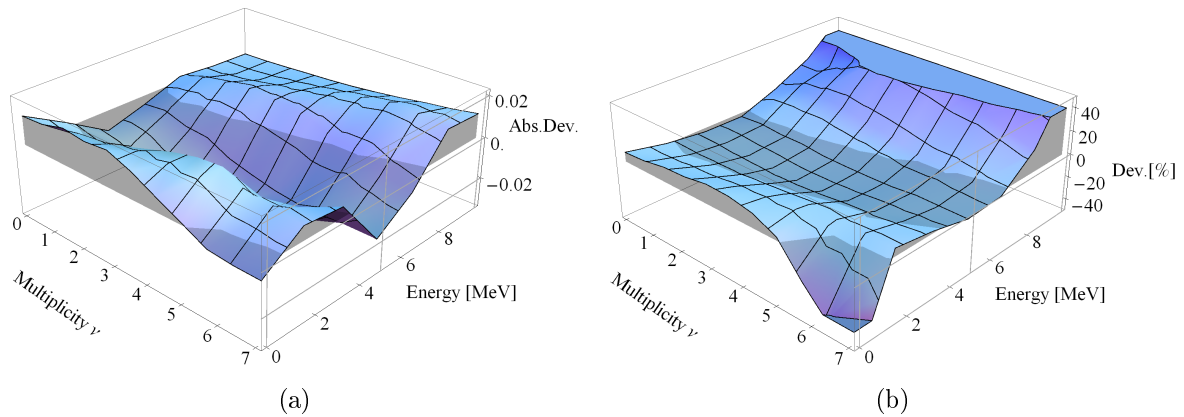


Figure B.2.: Dependence of the neutron-induced fission multiplicities  $P(\nu)$  on the incident energy  $E_n$  for  $^{235}\text{U}$ . The graphs show the absolute (a) and relative (b) difference between the analysis by Zucker and Holden [54] and calculations for the parameters of Terrell [37]. In this representation the data points (given only at integer values by [54]) are connected by a smooth function and the shaded area is the difference to zero. Relative deviations of more than  $\pm 40\%$  are reached only at very low values of  $P(\nu)$  and therefore not shown here.

Figure B.3.: Same as Figure B.2 but for  $^{238}\text{U}$ ; Relative deviations of more than  $\pm 20\%$  are reached only at very low values of  $P(\nu)$  and therefore not shown here.

